AD-A146 951 MODELING WAVE TRANSFORMATION IN THE SURF ZONE(U) 1/1
COASTAL ENGINEERING RESEARCH CENTER VICKSBURG MS
W R DALLY ET AL. SEP 84 CERC-MP-84-8

UNCLASSIFIED F/G 8/3 NL

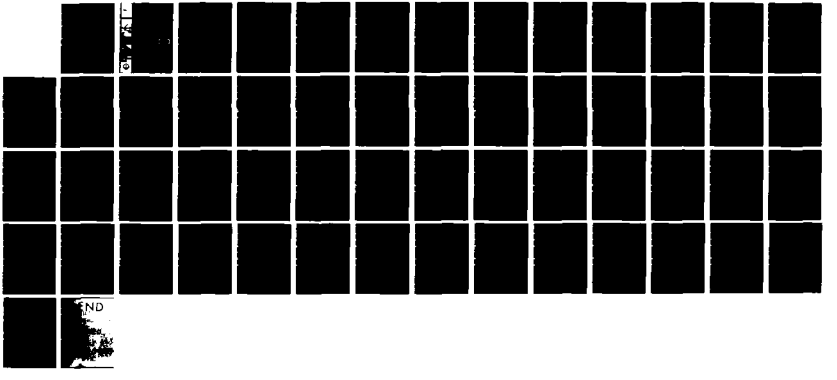

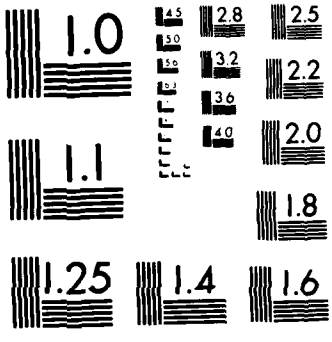

US Army Corps of Engineers

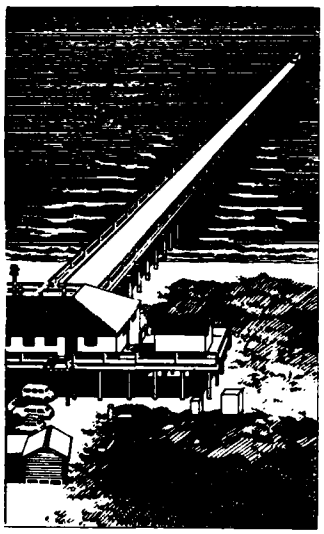

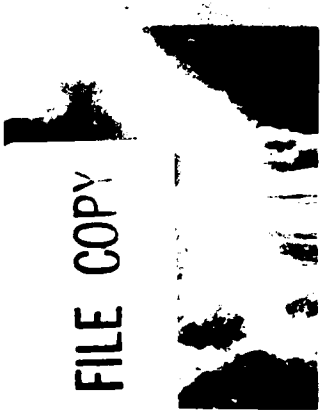

DTIC FILE COPY

(12)

MISCELLANEOUS PAPER CERC-84-8

MODELING WAVE TRANSFORMATION IN THE SURF ZONE

by

William R. Dally, Robert G. Dean,
Robert A. Dalrymple

Coastal Engineering Research Center

DEPARTMENT OF THE ARMY
Waterways Experiment Station, Corps of Engineers
PO Box 631
Vicksburg, Mississippi 39180-0631

September 1984
Final Report

Prepared for DEPARTMENT OF THE ARMY
US Army Corps of Engineers
Washington, DC 20314-1000
Under Work Unit C31551

Destroy this report when no longer needed. Do not return it to the originator.

The findings in this report are not to be construed as an official Department of the Army position unless so designated by other authorized documents.

The contents of this report are not to be used for advertising, publication, or promotional purposes. Citation of trade names does not constitute an official endorsement or approval of the use of such commercial products.

Unclassified

SECURITY CLASSIFICATION OF THIS PAGE *(When Data Entered)*

REPORT DOCUMENTATION PAGE		READ INSTRUCTIONS BEFORE COMPLETING FORM
1. REPORT NUMBER MISCELLANEOUS PAPER CERC-84-8	2. GOVT ACCESSION NO.	3. RECIPIENT'S CATALOG NUMBER
4. TITLE *(and Subtitle)* MODELING WAVE TRANSFORMATION IN THE SURF ZONE		5. TYPE OF REPORT & PERIOD COVERED Final report 6. PERFORMING ORG. REPORT NUMBER
7. AUTHOR(s) William R. Dally Robert G. Dean Robert A. Dalrymple		8. CONTRACT OR GRANT NUMBER(s)
9. PERFORMING ORGANIZATION NAME AND ADDRESS US Army Engineer Waterways Experiment Station Coastal Engineering Research Center PO Box 631, Vicksburg, Mississippi 39180-0631		10. PROGRAM ELEMENT, PROJECT, TASK AREA & WORK UNIT NUMBERS Work Unit Number C31551
11. CONTROLLING OFFICE NAME AND ADDRESS DEPARTMENT OF THE ARMY US Army Corps of Engineers Washington, DC 20314-1000		12. REPORT DATE September 1984 13. NUMBER OF PAGES 51
14. MONITORING AGENCY NAME & ADDRESS*(if different from Controlling Office)*		15. SECURITY CLASS. *(of this report)* Unclassified 15a. DECLASSIFICATION/DOWNGRADING SCHEDULE

16. DISTRIBUTION STATEMENT *(of this Report)*

Approved for public release; distribution unlimited.

17. DISTRIBUTION STATEMENT *(of the abstract entered in Block 20, if different from Report)*

18. SUPPLEMENTARY NOTES

Available from National Technical Information Service, 5285 Port Royal Road, Springfield, Virginia 22161.

19. KEY WORDS *(Continue on reverse side if necessary and identify by block number)*

Wave transformation	Numerical model
Wave decay	Surf zone
Wave breaking	Irregular bathymetry
Wave shoaling	Barred profiles

20. ABSTRACT *(Continue on reverse side if necessary and identify by block number)*

By drawing a macroscopic analogy between an idealized surf zone and a hydraulic jump, an expression for the spatial change in energy flux due to breaking is developed. Analytical solutions for wave height decay due to shoaling and breaking on a flat shelf and a plane beach are presented and the results compared with laboratory data from Horikawa and Kuo (1966). The agreement is good. Setdown/setup in mean water level, bottom friction losses,

(Continued)

DD FORM 1 JAN 73 1473 EDITION OF 1 NOV 65 IS OBSOLETE

Unclassified

SECURITY CLASSIFICATION OF THIS PAGE *(When Data Entered)*

20. ABSTRACT (Continued).

and bottom profiles of arbitrary shape are introduced next and the equations transformed for numerical solution. The model is calibrated and verified with laboratory data with good results for the wave decay, but not so favorable results for setup. A test run on a prototype scale profile containing three bar and trough systems demonstrates the model's ability to describe the shoaling, breaking, and wave reformation process. Bottom friction is found to play a negligible role in wave decay in the surf zone when compared with shoaling and breaking.

PREFACE

This study was authorized as a part of the Civil Works Research and Development Program by the Office, Chief of Engineers (OCE), US Army. The work was performed under the work unit C31551, Numerical Modeling of Shoreline Response to Coastal Structures, which is part of the Shore Protection and Restoration Program. Mr. J. H. Lockhart, Jr., was the OCE Technical Monitor.

This study was conducted from 1 October 1982 through 30 September 1983 by the Coastal Engineering Research Center (CERC) in conjunction with related scientific studies by Professors Robert G. Dean, University of Florida, and Robert A. Dalrymple, University of Delaware. This report represents a technical paper prepared to present the overall results of these efforts. The CERC portion of the study was under the general supervision of Dr. Robert W. Whalin, former Technical Director and present Chief of CERC; Dr. Lewis E. Link, Jr., Assistant Chief of CERC; Mr. Rudolph P. Savage, former Chief of the Research Division; Dr. James R. Houston, present Chief of the Research Division and Manager, Shore Protection and Restoration Program; Dr. Craig T. Everts and Mr. H. Lee Butler, former and present Chiefs of the Coastal Processes Branch; and Mr. William R. Dally, Hydraulic Engineer, and Dr. S. Rao Vemulakonda, Research Hydraulic Engineer, former and present Principal Investigators of the Numerical Modeling of Shoreline Response to Coastal Structures work unit. Professor Kiyoshi Horikawa of the University of Tokyo provided the laboratory data used in this work. Mr. Philip Vitale generated the three-dimensional and contour plots.

Commander and Director of WES during the conduct of this investigation and the preparation of this report was COL Tilford C. Creel, CE. Technical Director was Mr. F. R. Brown.

CONTENTS

	Page
PREFACE	1
PART I: INTRODUCTION	3
Statement of the Problem	3
Purpose of the Study	3
PART II: MODEL DEVELOPMENT	4
Literature Review	4
Theoretical Development	6
Analytical Solutions	12
Additional Factors	13
Numerical Solution	17
Calibration of the Model	21
PART III: RESULTS FOR LABORATORY CONDITIONS	28
Wave Height	28
Setup	33
PART IV: RESULTS FOR LARGE SCALE CONDITIONS	38
PART V: CONCLUSIONS AND RECOMMENDATIONS	41
REFERENCES	43
APPENDIX A: ANALYTICAL SOLUTIONS FOR THE BREAKING WAVE MODEL	A1
APPENDIX B: NOTATION	B1

MODELING WAVE TRANSFORMATION IN THE SURF ZONE

PART I: INTRODUCTION

Statement of the Problem

1. A major problem encountered in modeling nearshore wave-induced phenomena is the description of wave parameters subsequent to the initiation of wave breaking. Specifically, wave height and its spatial gradients generate or have direct impact on sediment mobilization and suspension, littoral currents (in both the alongshore and on/offshore directions), wave-induced setup, and forces on coastal structures. While the 0.78 criterion (ratio of breaker height to water depth = 0.78) appears to provide a reasonable prediction of incipient breaking on mildly sloping beaches, data from several investigators (Horikawa and Kuo 1966, Nakamura, Shiraishi, and Sasaki 1966, Street and Camfield 1966, Divoky, Le Méhauté, and Lin 1970) show that this criterion does not hold farther into the surf zone and that such a similarity model is more inappropriate on mild slopes - just where many coastal scientists assume it is most valid. Another shortcoming of this and many other representations developed to date is that they are not applicable on non-monotonic beach profiles such as those containing bar/trough formations.

Purpose of the Study

2. The purpose of this study is to develop a general numerical model for wave decay and transformation subsequent to breaking which includes the effects of bottom friction, wave-induced setup, and beach profiles of arbitrary shape. The model will be calibrated and verified with laboratory and prototype scale data.

PART II: MODEL DEVELOPMENT

Literature Review

3. During the past two decades a number of laboratory, field, and analytical studies have been conducted to develop a realistic model of wave height transformation across the surf zone. Such a model is essential to an adequate understanding of nearshore hydrodynamics and longshore sediment transport. The steady-state equation governing energy balance for waves advancing directly toward shore is*

$$\frac{\partial(EC_g)}{\partial x} = -\delta(x) \tag{1}$$

in which

E = wave energy per unit surface area

C_g = group velocity

x = horizontal coordinate normal to the beach and increasing toward the shore

δ = energy dissipation rate per unit surface area due to boundary shear, turbulence due to breaking, etc.

The central problem in previous studies has been the development of a rational and universally valid formulation for δ. The most physically appealing approach, first advanced by Le Méhauté (1962), has been the approximation of a breaking wave as a propagating bore (or hydraulic jump) in which case δ is given by

$$\delta = \frac{\rho g}{4} \frac{(BH)^3}{h^2} Q \tag{2}$$

where

ρ = mass density of water

g = acceleration due to gravity

---

* For convenience, symbols and unusual abbreviations are listed and defined in the Notation (Appendix B).

B = parameter representing the fraction of the wave height that is due to breaking

H = wave height

h = water depth

Q = transport of water across the bore

Since its first introduction by Le Méhauté, Equation 2 has been used in slightly different forms by a number of investigators to represent periodic water waves in the laboratory (Divoky, Le Méhauté, and Lin (1970), Hwang and Divoky (1970), Svendsen, Madsen and Hansen (1978)), aperiodic water waves in the laboratory (Battjes and Janssen (1978)), and aperiodic waves in nature (Thornton and Guza (1983)).

4. Other approaches for wave energy dissipation have included that of Horikawa and Kuo (1966) in which the internal energy dissipation is represented in terms of turbulent velocity fluctuations which are assumed to decay exponentially with distance from the wave break point. In a different approach, Mizuguchi (1980) applies the analytical solution of Lamb (1932) for internal energy dissipation due to viscosity, replacing the molecular kinematic viscosity with eddy viscosity which must be estimated based on the wave and beach profile characteristics.

5. Understandably, the extension of approaches developed for periodic waves to aperiodic waves introduces complexities, primarily with respect to representation of the probability distribution function. In a laboratory study of breaking random waves over plane and barred beaches, Battjes and Janssen (1978) employed Equation 2 interpreting H as H_{rms} and introduced two assignable constants. A truncated Rayleigh wave height distribution was assumed with a finite probability of the maximum truncating wave height occurring, resulting in a delta function at this limit. Battjes and Janssen included the effect of wave setup and demonstrated good agreement between the predicted and the measured wave height distribution. Following Collins (1970), Kuo and Kuo (1974) modified the truncated wave height probability distribution by omitting the delta function at the upper wave height. Goda (1975) adopted a modified probability distribution in which the distribution decreases linearly to zero over a specified upper range of the wave heights. Based on field measurements, Thornton and Guza (1983) present convincing data that the unmodified Rayleigh distribution is applicable seaward of and across

the entire surf zone. At each location, they define a breaking subpopulation of the waves.

6. In the course of the investigations described above, a substantial data base of wave height transformation across laboratory and field beaches of various profiles has been developed. Nakamura, Shiraishi and Sasaki (1966) presented data based over 1500 runs of wave transformation across a plane beach in the laboratory. This assemblage of wave data is useful in providing guidance and a basis for evaluation in an attempt to develop a universally valid model.

7. None of the models developed and evaluated to date provide a demonstrated, completely general capability for representing wave transformation across the surf zone. The waves in this zone are not linear and some of the difficulty may be in the application of linear theory, although other theories (cnoidal and solitary) have been used by some investigators.

8. One of the features not represented in most models is that of the wave height stabilizing at some value in a uniform depth following the initiation of breaking. The laboratory data of Horikawa and Kuo (1966) and general observations and intuition support such a phenomenon, yet none of the energy dissipation models based on the moving hydraulic jump predicts this effect. Although the model by Mizuguchi (1980) includes this stabilization, a simpler model could minimize the difficulties in estimating the representative eddy viscosity and in rationally applying the model to a beach of nonuniform slope.

9. This report centers on the development and evaluation of a model which includes the wave height stabilization and which appears to be broadly applicable based on comparison with periodic water wave data from laboratory studies. In comparison with the laboratory data, the available field data are much more limited. The evaluation of a model by laboratory data would further an understanding of the problem.

Theoretical Development

10. The primary purpose of this work is to accurately describe the decay in wave height due to breaking as a wave crosses the surf zone. Ultimately, it is desirable to address as much of the wave transformation process as possible, including shoaling, breaking, and reformation. Due to the complexity of the problem, a common approach is to draw an analogy between the turbulent

front face of a breaking wave and a moving hydraulic jump (Le Méhauté (1962), Peregrine and Svendsen (1978)). However, in the present model a more macroscopic treatment is applied where the energy dissipation across the entire surf zone is compared to that of a hydraulic jump. Rather than attempting to quantify the local energy dissipation by addressing the turbulent velocity fluctuations, a common method is to describe the local gradient in depth-integrated energy flux as stated in Equation 1. In the typical hydraulic jump in a rectangular channel (Figure 1a), energy is dissipated over some distance to transform a high energy condition (Froude Number $F > 1$) to a lower energy condition ($F < 1$) by way of turbulence. The specific energy (energy per unit weight) of the flow anywhere along the channel as introduced by Bakhmeteff in 1912 is given by

$$E' = h + \frac{u^2}{2g} \tag{3}$$

where it is assumed that the horizontal fluid velocity u is uniform over the depth of flow h. The energy per unit volume is then

$$E = \gamma h + \frac{\rho u^2}{2} \tag{4}$$

where γ is the unit weight. The energy flux per unit width of the channel past any section is given by

$$E_{Flux} = Euh = \gamma u h^2 + \frac{\rho u^3 h}{3} \tag{5}$$

Defining the flow rate per unit width of channel, which is spatially and temporally constant, as $q = uh$, Equation 5 becomes

$$E_{Flux} = \gamma q h + \frac{\rho q^3}{2h^2} \tag{6}$$

The local rate of energy dissipation per unit plan area is simply the spatial gradient of the energy flux

$$\frac{dE_{Flux}}{dx} = \left(\gamma q \frac{h}{2} - \frac{\rho q^3}{2h^2}\right) \frac{2}{h} \frac{dh}{dx} \tag{7}$$

which can also be written as

$$\frac{dE_{Flux}}{dx} = - \left[\left(\gamma qh + \frac{\rho q^3}{2h^2}\right) - \frac{3}{2} \gamma qh\right] \frac{2}{h} \frac{dh}{dx} \tag{8}$$

The term in parentheses in Equation 8 is the local energy flux as previously defined by Equation 6. The second term in the brackets is equivalent to the energy flux that would be present if the flow were critical ($F = 1$) at that location. Moreover, if the flow were critical, this would be the minimum energy flux that would occur for the given flow rate. Equation 8 is then

$$\frac{dE_{Flux}}{dx} = \frac{-2 \frac{dh}{dx}}{h} \left(E_{Flux} - E_{Flux_{"min"}}\right) \tag{9}$$

The local slope of the water surface dh/dx cannot be determined without a knowledge of the details of the vertical flow regime within the jump. Fortunately, it is the form of Equation 9 that will be of interest when the breaking wave case is addressed.

11. Next, consider a beach profile that rises from deep water in a gently sloping manner and at some point in shallow water becomes horizontal (see Figure 1b). Consider further a wave propagating onto this profile with characteristics such that breaking starts at the point where the bottom becomes horizontal. The wave will not instantaneously stop breaking because the bottom has become horizontal (as dictated by the 0.78 criterion) but would continue to break until some stable wave height is attained. Breaking would be most intense just shoreward of line AA and would decrease until an approximate stable wave height is reached at line BB. This idealized surf zone can be thought of as an elongated hydraulic jump, where again, a high energy free surface flow condition is converted to a lower energy one by the dissipation of energy through turbulence. In both situations, it appears that the fluid

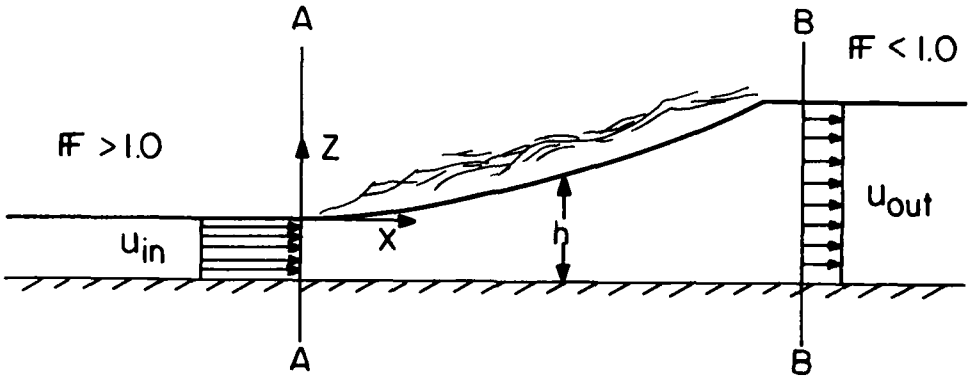

a. Typical hydraulic jump

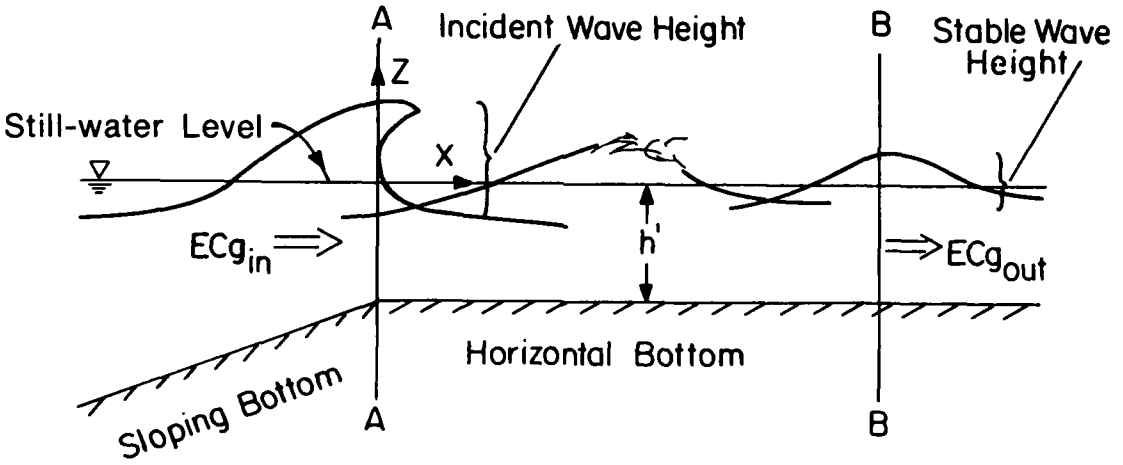

b. Idealized surf zone

Figure 1. Analogy between idealized surf zone and hydraulic jump

flow surpasses some criterion and then dissipates energy until the end result is a flow condition well below the criterion. (For the hydraulic jump, this criterion is $F = 1$, but if such a criterion exists for breaking waves, it is heretofore unresolved.) For these reasons, the following expression, similar to Equation 9, will be used to describe energy dissipation across the surf zone:

$$\frac{d(ECg)}{dx} = \frac{-K}{h'}\left[ECg - (ECg)_s\right] \tag{10}$$

Here

ECg = depth-integrated time-averaged energy flux as given by shallow water linear wave theory

K = dimensionless decay coefficient

h' = still-water depth

ECg_s = energy flux associated with the "stable" wave condition that the breaking wave is striving to attain

Horikawa and Kuo (1966) conducted laboratory tests with a bottom configuration identical to the one described. As shown in Figure 2, their data indicate a stable wave criterion given by

$$H_s = \Gamma h' \tag{11}$$

where

H_s = stable wave height

Γ = dimensionless coefficient whose value appears to lie somewhere between 0.35 and 0.40

12. In Figure 3, wave height was plotted against still-water depth for a uniform beach slope of 1/65, revealing that the breaking waves tended to approach asymptotically the line $H = 0.5h'$ where H is the local wave height. Equation 11 appears to be a reasonable assumption, and Equation 10 can then be written as

$$\frac{d[H^2(h')^{1/2}]}{dx} = \frac{-K}{h'}[H^2(h')^{1/2} - \Gamma^2(h')^{5/2}] \tag{12}$$

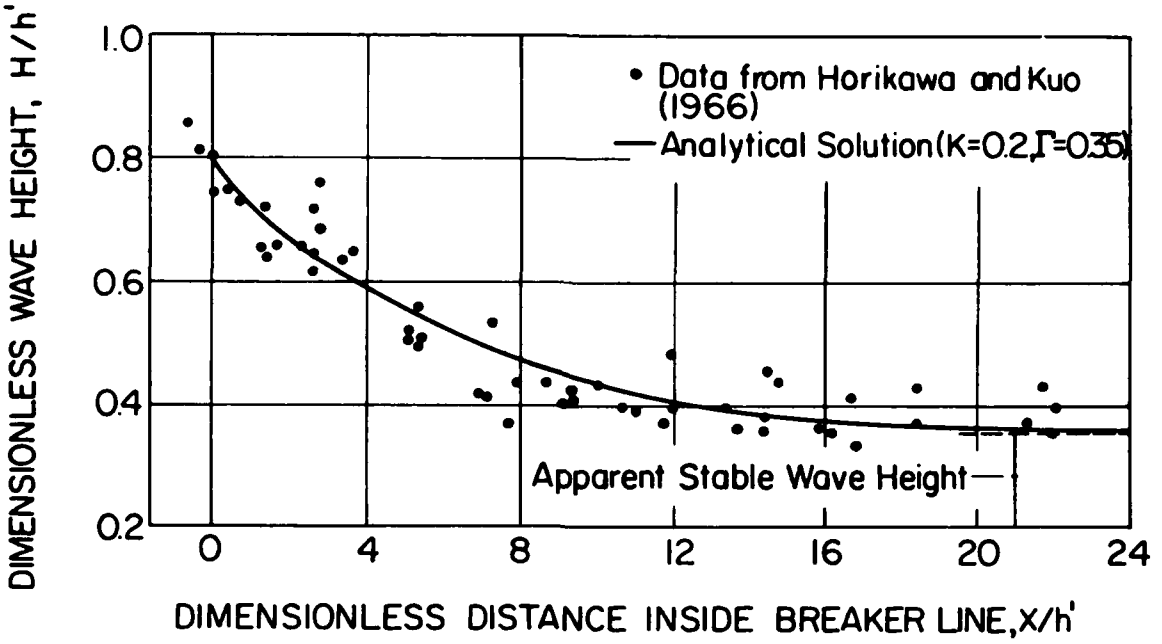

Figure 2. Comparison of analytical solution (Equation 13) with experimental results of Horikawa and Kuo for waves breaking on a shelf

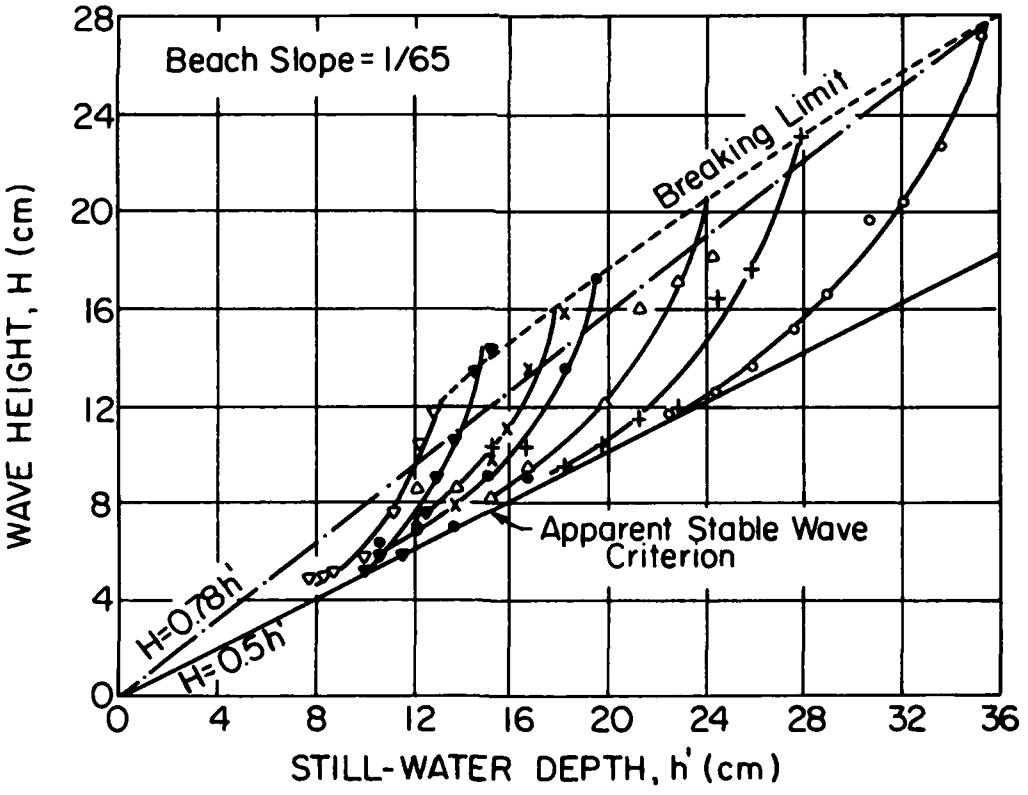

Figure 3. Wave decay on a 1/65 slope as presented in Horikawa and Kuo (1966) and the apparent stable wave criterion

where C_g is taken as $\sqrt{gh'}$. It should be noted that Equations 10, 11, and 12 can be applied to a bottom of varying depth and slope because shoaling is included implicitly. (If $K = 0$, the model reverts to conservation of energy.)

Analytical Solutions

Horizontal bottom

13. For the special beach shown in Figure 1b, Equation 12 can be solved analytically if setup in the mean water level is neglected as shown in Appendix A. The decay in wave height in the surf zone is given by

$$\frac{H}{h'} = \left(\left\{ \left[\left(\frac{H}{h'} \right)_b^2 - \Gamma^2 \right] \exp\left(-K \frac{x}{h'} \right) \right\} + \Gamma^2 \right)^{1/2} \tag{13}$$

where the subscript b denotes conditions at incipient breaking and x has its origin at the breaker line and is directed onshore. This expression dictates that the energy flux will decay exponentially across the surf zone, never quite reaching the stable wave state known to exist. However, Equation 13 may still be pertinent because energy dissipated by internal and bottom friction could account for the difference between the wave height predicted by Equation 13 and the stable wave height. Note that if $K = 0$, the wave height remains constant, as would be expected. Equation 13 is plotted in Figure 2 with $K = 0.2$, $\Gamma = 0.35$, and $(H/h')_b = 0.8$.

Plane beach

14. Equation 12 also can be solved analytically for the case of a beach of uniform slope (Appendix A). Again neglecting setup, the decay in wave height across the surf zone is given by

$$\frac{H}{H_b} = \left[\left(\frac{h'}{h'_b} \right)^{[(K/m)-1/2]} (1 + \alpha) - \alpha \left(\frac{h'}{h'_b} \right)^2 \right]^{1/2} \tag{14}$$

in which m is the beach slope, and

$$\alpha = \frac{K\Gamma^2}{m\left(\frac{5}{2} - \frac{K}{m}\right)} \left(\frac{h_b'}{H_b}\right)^2 \tag{15}$$

Note that this solution fails when $K/m = 5/2$. For this special case, the solution is

$$\frac{H}{H_b} = \left(\frac{h'}{h_b'}\right)\left[1 - \beta \ell n \left(\frac{h'}{h_b'}\right)\right]^{1/2} \tag{16}$$

where

$$\beta = \frac{5}{2} \Gamma^2 \left(\frac{h_b'}{H_b}\right)^2 \tag{17}$$

Also note that if K is set equal to zero (no decay), Equation 14 becomes

$$\frac{H}{H_b} = \left(\frac{h_b'}{h'}\right)^{1/4} \tag{18}$$

which is Green's Law. If $\alpha = -1.0$, Equation 14 reverts to the common similarity model $H \propto h'$. Equations 14 and 16 are plotted in Figures 4a and 4b for several values of H_b/h_b' and K/m . Figure 5 compares Equation 14 with the data presented in Horikawa and Kuo (1966).

Additional Factors

Setup

15. During initial examination of the complete raw data set collected by Horikawa and Kuo, it was noticed that in all cases where measurements were taken in the inner portion of the surf zone, as the still-water depth approached zero the wave height did not (Figure 5). To model this phenomenon

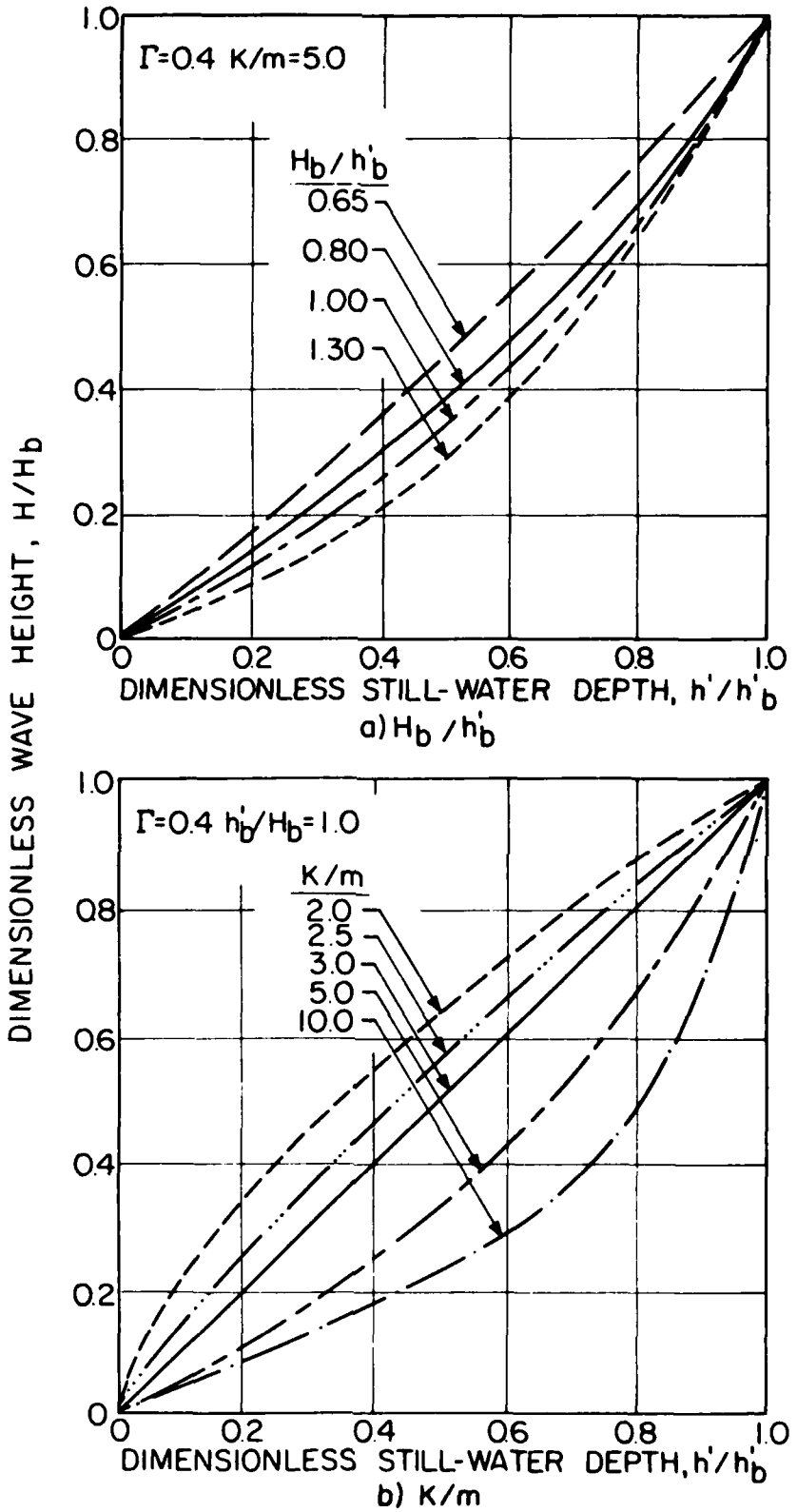

Figure 4. Dependence of analytical solution (Equations 14 and 16) on H_b/h'_b and K/m for waves breaking on a plane beach

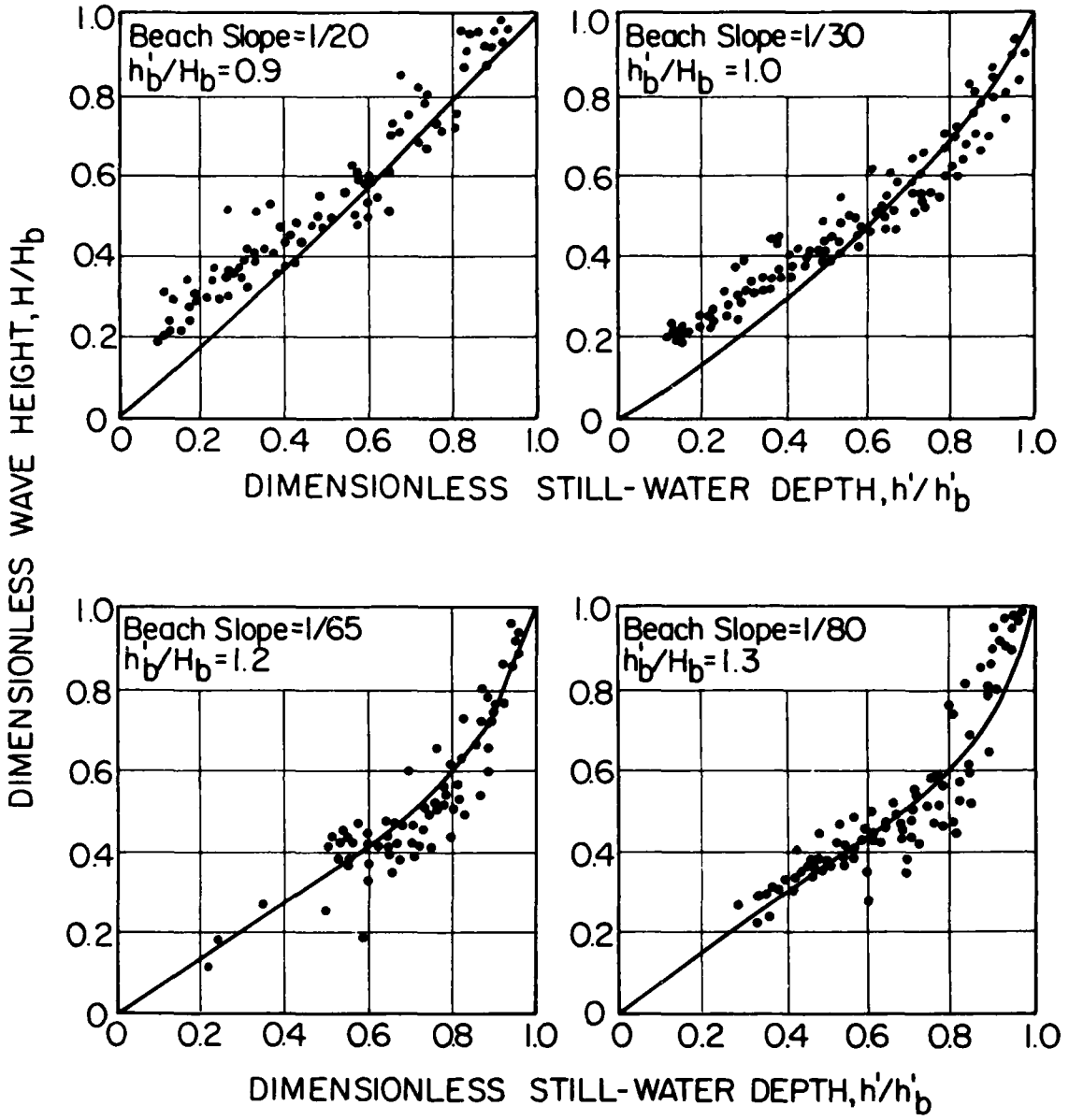

Figure 5. Comparison of analytical solution (Equation 14) with wave decay data as presented in Horikawa and Kuo (1966) for various beach slopes ($K = 0.17$, $\Gamma = 0.5$)

better, wave-induced setup and setdown of the mean water level must be included. The same conclusion was reached originally by Hwang and Divoky (1970). From Longuet-Higgins and Stewart (1963), the slope of the mean water level $\bar{\eta}$ is given by

$$\frac{d\bar{\eta}}{dx} = \frac{-1}{\rho g(h' + \bar{\eta})} \frac{dS_{xx}}{dx} \tag{19}$$

where the radiation stress S_{xx} in shallow water is

$$S_{xx} = \frac{3}{16} \rho g H^2 \tag{20}$$

Equation 19 becomes

$$\frac{d\bar{\eta}}{dx} = \frac{-3}{16} \frac{1}{(h' + \bar{\eta})} \frac{dH^2}{dx} \tag{21}$$

and can be used in conjunction with a slightly different form of Equation 10

$$\frac{d(ECg)}{dx} = \frac{-K}{h} [ECg - (ECg)_s] \tag{22}$$

and Equation 12

$$\frac{d[H^2(h)^{1/2}]}{dx} = \frac{-K}{h} [H^2(h)^{1/2} - \Gamma^2(h)^{5/2}] \tag{23}$$

in which h, the mean water depth given by

$$h = h' + \bar{\eta} \tag{24}$$

has replaced the still-water depth h'.

Bottom friction

16. Although energy dissipation due to bottom friction is generally negligible when compared to energy loss due to breaking, the former will be examined in this paragraph. The average rate of energy dissipation per plan area due to bottom friction is expressed by

$$E_{LB} = \frac{1}{T} \int_0^T \tau_B u_B dt \tag{25}$$

where T is the wave period, τ_B is the bottom shear stress given by

$$\tau_B = \rho \frac{f}{2} u_B |u_B| \tag{26}$$

and u_B is taken to be the first-order horizontal water particle velocity at the bottom which (from linear wave theory in shallow water) is

$$u_B = \frac{H}{2} \sqrt{\frac{g}{h}} \cos \sigma t \tag{27}$$

and t is the time.

f = drag coefficient dependent on flow and bottom/sediment characteristics

σ = wave angular frequency

Substituting Equations 26 and 27 into Equation 25 and integrating yields

$$E_{LB} = \frac{\rho f H^3}{12\pi} \left(\frac{g}{h}\right)^{3/2} \tag{28}$$

Numerical Solution

17. Introducing setup, beach profiles of more realistic shape, or bottom friction to the model render the equations unsolvable analytically. A numerical scheme will therefore be developed which describes the one-dimensional transformation of wave height over bottoms of arbitrary shape due to shoaling, breaking, reformation, and bottom friction, including the effects of setup in mean water level.

18. Rewriting Equation 22 in a finite difference form using a central average for each of the quantities on the right-hand side gives

$$\frac{(\tilde{ECg})_{i+1} - (ECg)_i}{\Delta x} = \frac{-K}{h_m} \left[\frac{(\tilde{ECg})_{i+1} + (ECg)_i}{2} - \frac{(ECg)_{s_{i+1}} + (ECg)_{s_i}}{2} \right] \quad (29)$$

where

$$h_m = \frac{h_i + h_{i+1}}{2} = \frac{h'_i + \bar{\eta}_i + h'_{i+1} + \bar{\eta}_{i+1}}{2} \quad (30)$$

and the superscript (~) denotes conditions before bottom friction is applied. By applying shallow-water wave theory and the stable wave criterion $H_s = \Gamma h$ Equation 29 may be transformed to

$$\tilde{H}_{i+1} = \left[\frac{(1 - \lambda)}{(1 + \lambda)} H_i^2 \left(\frac{h_i}{h_{i+1}} \right)^{1/2} + \frac{\lambda}{(1 + \lambda)} \left(\Gamma^2 h_{i+1}^2 + \Gamma^2 \frac{h_i^{5/2}}{h_{i+1}^{1/2}} \right) \right]^{1/2} \quad (31)$$

in which

$$\lambda = \frac{K\Delta x}{2h_m} \quad (32)$$

Equation 21 is treated in a similar manner

$$\bar{\eta}_{i+1} = \frac{-3}{16} \frac{\tilde{H}_{i+1}^2 - H_i^2}{h_m} + \bar{\eta}_i \quad (33)$$

Before $\tilde{H}_{i+1}$ can be calculated, the mean water level at i+1 must be known. The assumption is made that the mean water depth at the next location can be approximated by

$$h_{i+1} \simeq h'_{i+1} + \bar{\eta}_i \quad (34)$$

A first estimate of $\tilde{H}_{i+1}$ can be obtained using Equation 31, after which a better estimate of h_{i+1} is made using Equation 33. The program iterates until the new value for the mean water depth is very close to the old one. In the calibration runs, no more than three iterations were required for the difference in estimates to become less than a millimeter.

19. The decay in wave energy due to bottom friction is not included directly in the wave height computation but is calculated separately using Equation 28 and energy flux considerations. This procedure yields

$$H_{i+1} = \left[\tilde{H}_{i+1}^{2} - \frac{2f\Delta x}{3\pi h_m^{3/2} h_{i+1}^{1/2}} \left(\frac{\tilde{H}_{i+1} + H_i}{2} \right)^3 \right]^{1/2} \tag{35}$$

where H_{i+1} is the wave height at the next point of interest after shoaling, breaking, and bottom friction have been applied. Separating the bottom friction in this manner is justified because it plays a significant role only in the absence of breaking.

20. To apply the model in a given situation, the following information is required: (a) the wave height and still-water depth at a known nearshore location, (b) the ratio of wave height to water depth at incipient breaking, (c) the bottom friction coefficient, and (d) the bottom profile. The ratio of breaking height to depth is not easily predicted and was not treated in an extensive manner in this study. Mallard (1978) offers a more complete investigation. Assuming the starting point is in shallow water and outside the surf zone, the setdown in mean water level as given by Longuet-Higgins and Stewart (1963) is

$$\bar{\eta}_1 = \frac{-H_1^2}{16h_1} \tag{36}$$

21. From these initial conditions and using Equations 31, 33, and 35 as described, the wave height will increase (with some loss in height due to bottom friction) as the wave moves shoreward until the incipient breaking criterion is reached. The wave then breaks until it becomes locally stable

(if at all). On barred profiles, the combination of wave decay and increasing water depth as the wave passes over the trough enables the wave to reach stability. The "reformed" wave then shoals again until the breaking criterion is reached and the process repeats until the mean water depth reaches an arbitrarily chosen small value (0.25 m is a reasonable choice at prototype scale). A flow chart of the wave transformation model is shown in Figure 6.

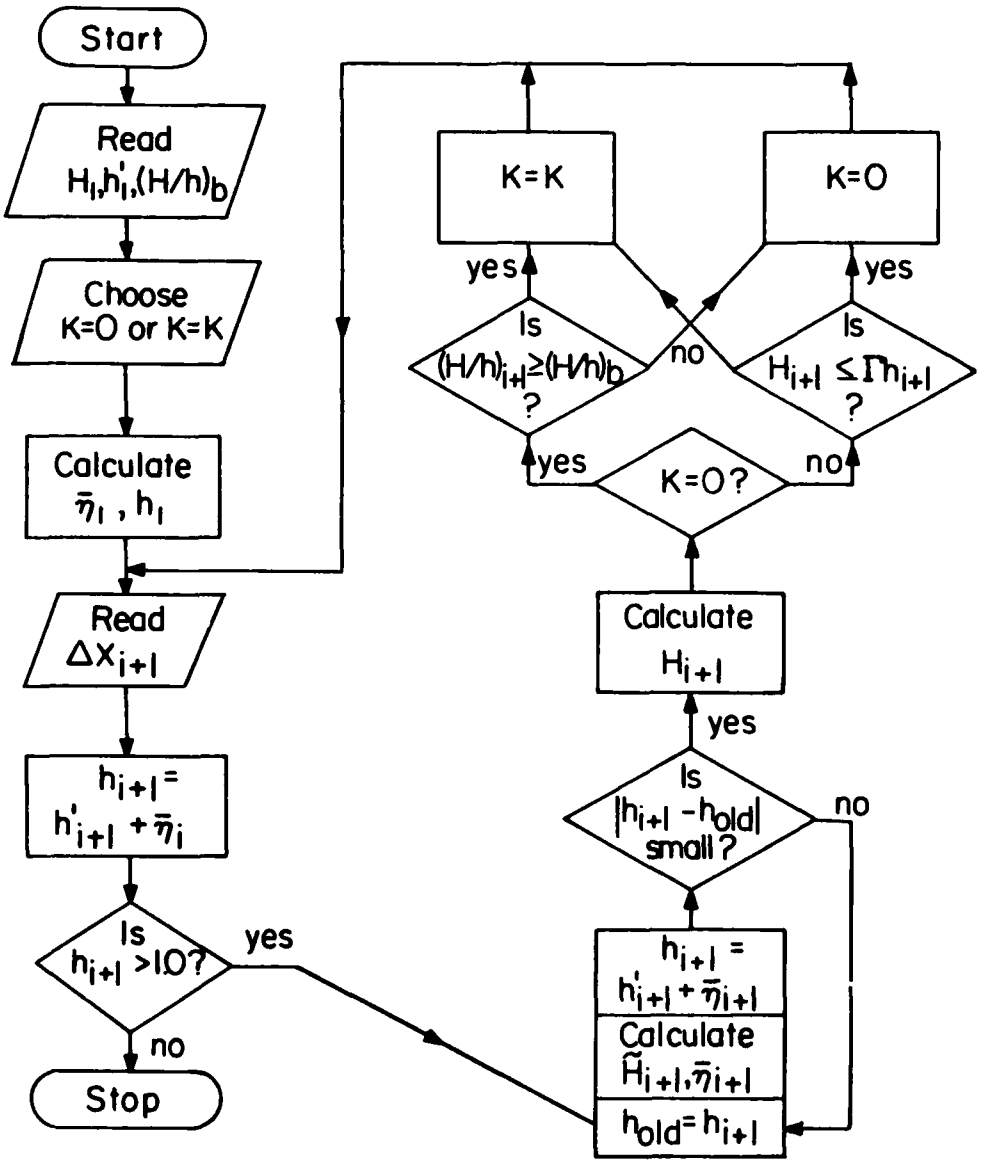

Figure 6. Flow chart of wave transformation model (Equations 31, 33, and 35) which includes shoaling, breaking, reformation, bottom friction, and setup

Calibration of the Model

22. The model is calibrated by determining the best values for the stable wave factor (Γ) and the wave decay factor K using a least-squares procedure. Horikawa and Kuo's (1966) original laboratory data of waves breaking on plane slopes were examined. Starting at incipient breaking, the location of wave heights were measured by Horikawa and Kuo at known distances across the surf zone under monochromatic wave conditions for plane smooth beaches of rubber and concrete having slopes of 1/20, 1/30, 1/65, and 1/80. The wave period varied from 1.2 to 2.2 sec and the incipient breaker height from 7 to 27 cm. Although not specifically stated by Horikawa and Kuo, the breakers must have spanned both the plunging and spilling types because the ratio of wave height to water depth at incipient breaking ranged from 0.63 to 1.67. The number of waves and data points for the slopes analyzed are presented as follows:

Slope	Number of Waves	Number of Data Points
1/30	17	173
1/65	12	96
1/80	56	500

Data from the 1/20 slope were not included in the calibration because the measurements were made too far apart for the model to remain numerically stable. The error function to be minimized is defined by

$$\varepsilon(\Gamma, K) = \left\{ \frac{\sum_{j=1}^{N} [H_{pj}(\Gamma, K) - H_{mj}]^2}{\sum_{j=1}^{N} H_{mj}^2} \right\}^{1/2} \tag{37}$$

where

H_{mj} = measured wave height

H_{pj} = wave height at that location as predicted by the numerical scheme for given incipient conditions and values of Γ and K

N = number of data points analyzed

A lengthy and involved attempt to obtain best-fit values of Γ and K was made using a nonlinear, least-squares error analysis. This method involves choosing initial values for the factors, fitting a parabolic surface to the error surface at that point, locating the minimum of the fitted surface, and using these new values of Γ and K for the next attempt. In this manner, the procedure theoretically converges on the minimum of the error surface. However, this method was unsuccessful, apparently because the error surfaces are too highly nonlinear, i.e., a paraboloid is a poor approximation for the error surface. By calculating the error at regular intervals of K and Γ, a discretized error surface can be generated, its low point occurring near the best- fit values for the factors. Figures 7, 8, and 9 display three-dimensional and contour plots of the error surfaces for the data taken on the 1/30, 1/65, and 1/80 slopes. Note the recurved shapes of all the surfaces and the saddle point present in two of the contour plots. A one-wave, sixteen-point artificial "data" set was generated using the model on a 1/80 slope with Γ set equal to 0.35 and K equal to 0.10 (the best fit values from the real 1/80 data set). Figure 10 displays the corresponding error surface and contour plots. Note that it has the same general shape and saddle point as the real data set. It can therefore be concluded that the shape and saddle point are characteristics of the model and are not due to problems with the data set. The best fit values for Γ and K for the three slopes analyzed are presented as follows:

Slope	Γ	K	Minimum Error
1/30	0.475	0.275	0.1165
1/65	0.355	0.115	0.1049
1/80	0.350	0.100	0.1298

The best-fit values for the two factors do vary with beach slope, especially as the beach becomes steeper. However, it would be preferable to choose single values for Γ and K which give satisfactory results for all beach slopes, allowing the model to be used on beach profiles of more realistic shape. Fortunately, the error surfaces for the three slopes tested are relatively broad and flat in the vicinity of their minima, so the factors can be changed without excessively increasing the combined error. The procedure

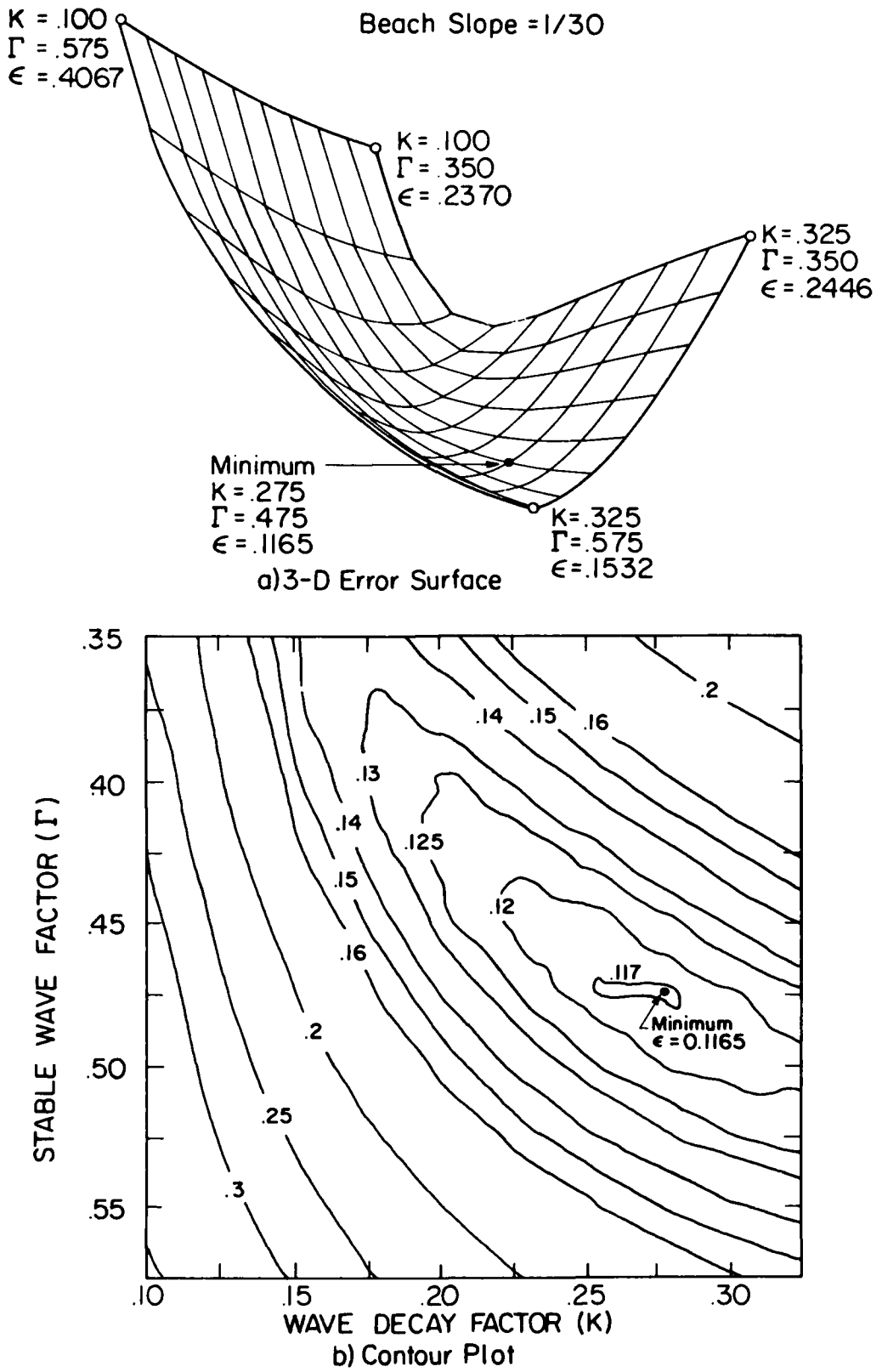

Figure 7. Three-dimensional and contour plots of error ε between numerical solution and laboratory data as a function of wave decay factor K and stable wave factor Γ for 1/30 beach slope

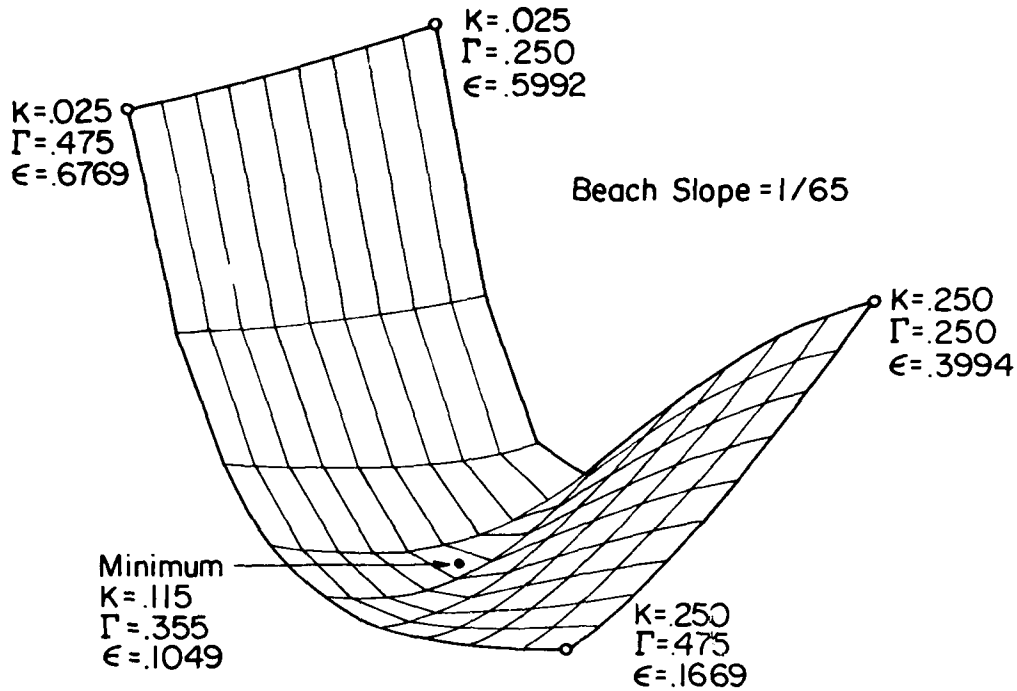

a) 3-D Error Surface

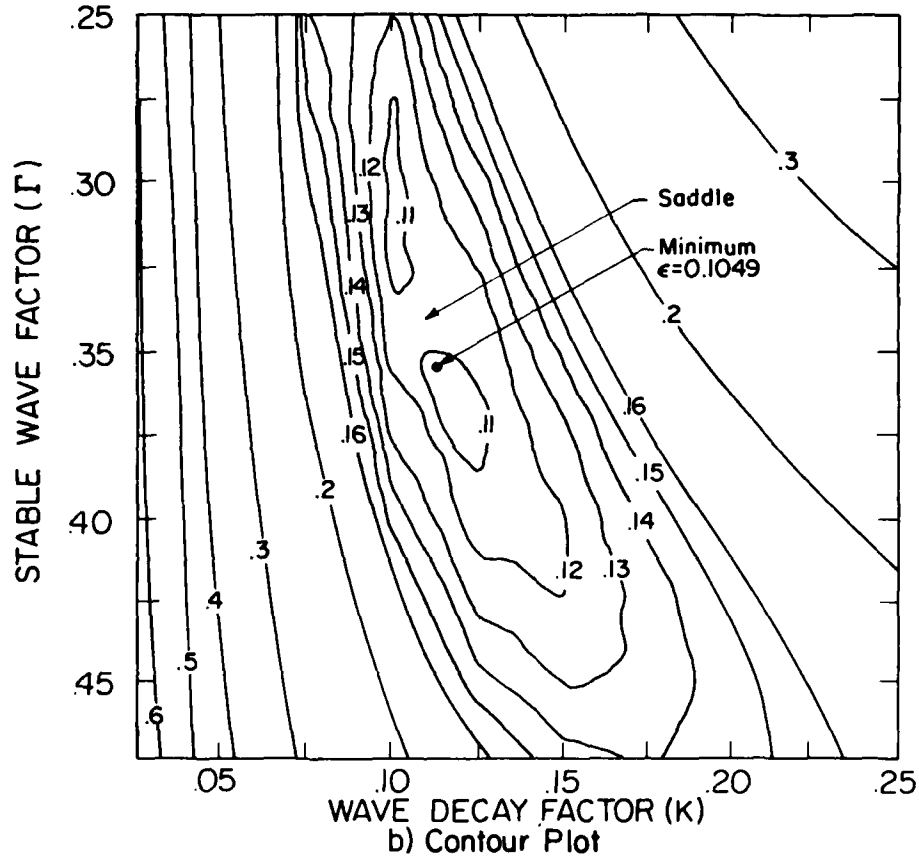

b) Contour Plot

Figure 8. Three-dimensional and contour plots of error ε between numerical solution and laboratory data as a function of wave decay factor K and stable wave factor Γ for 1/65 beach slope

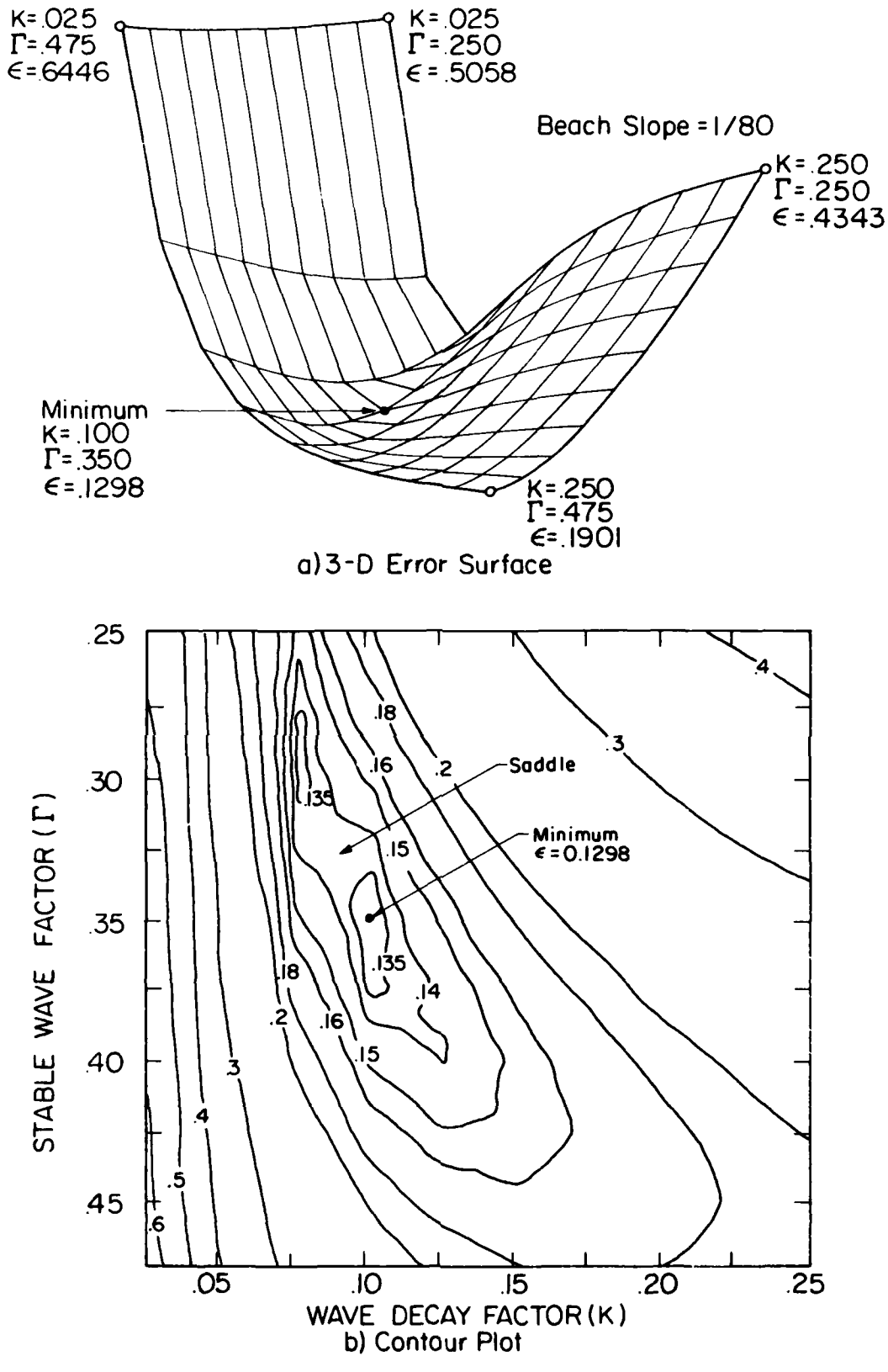

Figure 9. Three-dimensional and contour plots of error ϵ between numerical solution and laboratory data as a function of wave decay factor K and stable wave factor Γ for 1/80 beach slope

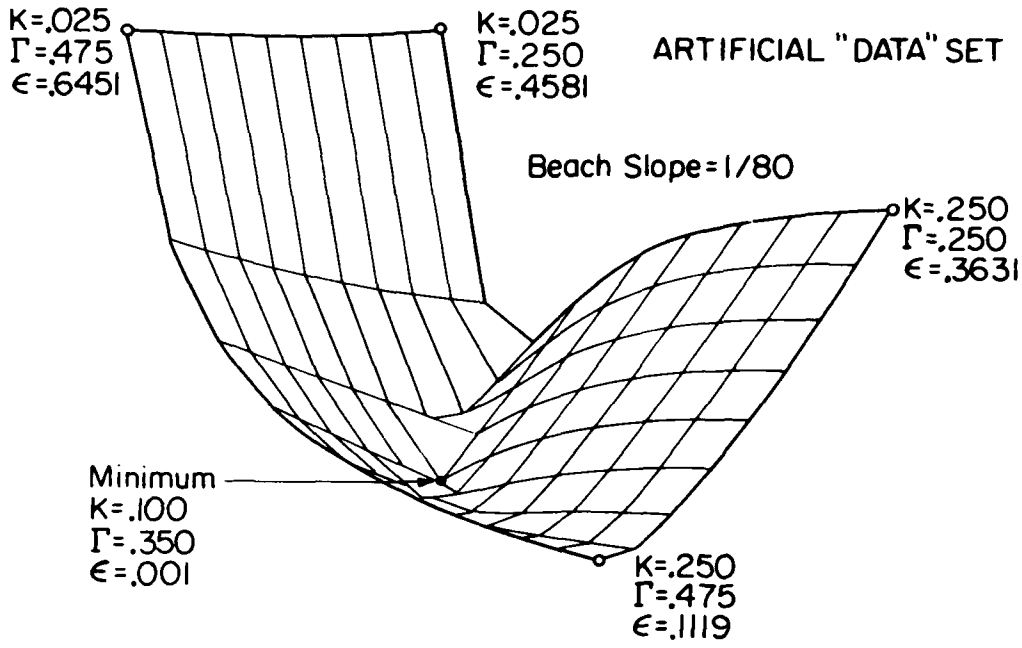

a) 3-D Error Surface

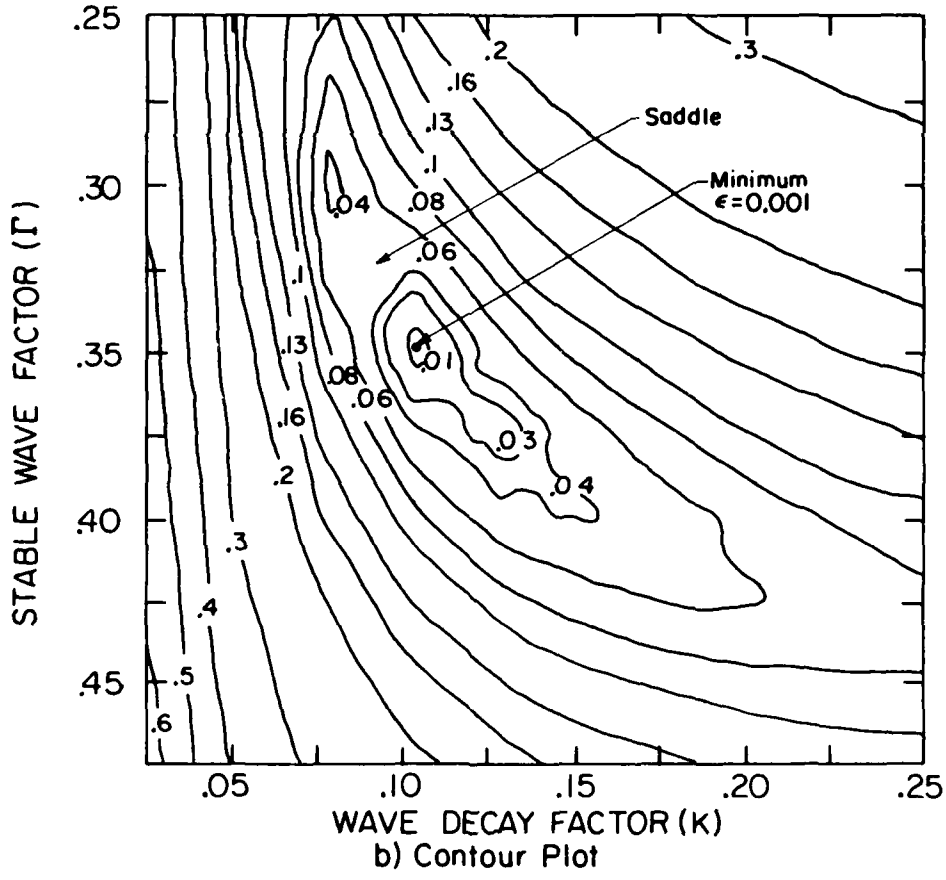

b) Contour Plot

Figure 10. Three-dimensional and contour plots of error ϵ between numerical solution and model-generated "data" as a function of wave decay factor K and stable wave factor Γ for 1/80 beach slope

followed was to superimpose the contour plots of Figures 7, 8, and 9 and find the location where the sum of the three error values is minimized. This point occurs at

$$\Gamma = 0.40$$

$$K = 0.15$$

and it is recommended that these values be used in situations where the bottom slope varies over a wide range. If the beach is nearly planar, the best-fit values presented for Γ and K for the three slopes may be used accordingly.

23. The breaker model was not calibrated to prototype conditions due to a lack of suitable data. It would require the measurement of the breaker height distribution across the surf zone under truly monochromatic conditions. The waves should be incident normal to the bottom contours, and the beach profile must be known and preferably monotonic. A large wave tank with a regular wave generator would be ideal for this type of experiment. Calibration of the model in its present form using irregular waves would require following each individual breaker as it travels across the surf zone (provided wave-wave interaction is not significant). Because the bubbles which dissipate the energy in breaking waves may not be scaled down properly in the laboratory, it is hypothesized that K will assume a lesser value under prototype conditions. It is unclear what change, if any, would occur in Γ.

PART III: RESULTS FOR LABORATORY CONDITIONS

Wave Height

24. Figures 11-14 display a representative sample of model-predicted breaker decay as compared with the aforementioned laboratory data for plane beaches of slopes 1/20, 1/30, 1/65, and 1/80. The figures are dimensional plots of wave height versus still-water depth. In all cases, the wave decay factor K was set equal to 0.15 and the stable wave factor Γ was taken to be 0.40. Bottom friction was considered negligible. Each curve was generated by taking as input the wave height and still-water depth at incipient breaking as given in the data and by calculating stepwise ($\Delta x = 1/m$)* the setup and decay profiles. It is not practical to display the data and model results in dimensionless form due to the dependency of the shape of the decay profile on the incipient conditions as well as the setup. Moreover, setup measurements were not included in the Horikawa and Kuo experiments.

25. Examination of these results shows that the model developed in this study appears to provide a good representation of breaking wave decay on plane beaches of laboratory scale. It is important to note that the model is in good quantitative agreement over the wide range of slopes tested, even with the two factors K and Γ held constant at values that are not necessarily the best-fit values for that particular slope.

26. The line $H = 0.78\ h'$ is plotted in each of the figures and appears to be a reasonable description of breaker decay for only the 1/30 slope. In fact, the surf similarity model ($H \propto h'$) which is so prevalent in the coastal literature seems to be remotely valid only for beaches of much greater slope than those commonly found in nature.

27. For waves having similar ratios of incipient breaker height to depth but different incipient breaker heights, the measured decay profiles intersect. This phenomenon is apparent also in the profiles produced by the model. The greater total setup associated with an initially larger wave (Bowen 1969) provides a greater mean water depth and so a larger stable wave height in the inner surf zone. At this point the larger wave decays less rapidly, causing the decay profiles to intersect.

---

* See notation (Appendix B).

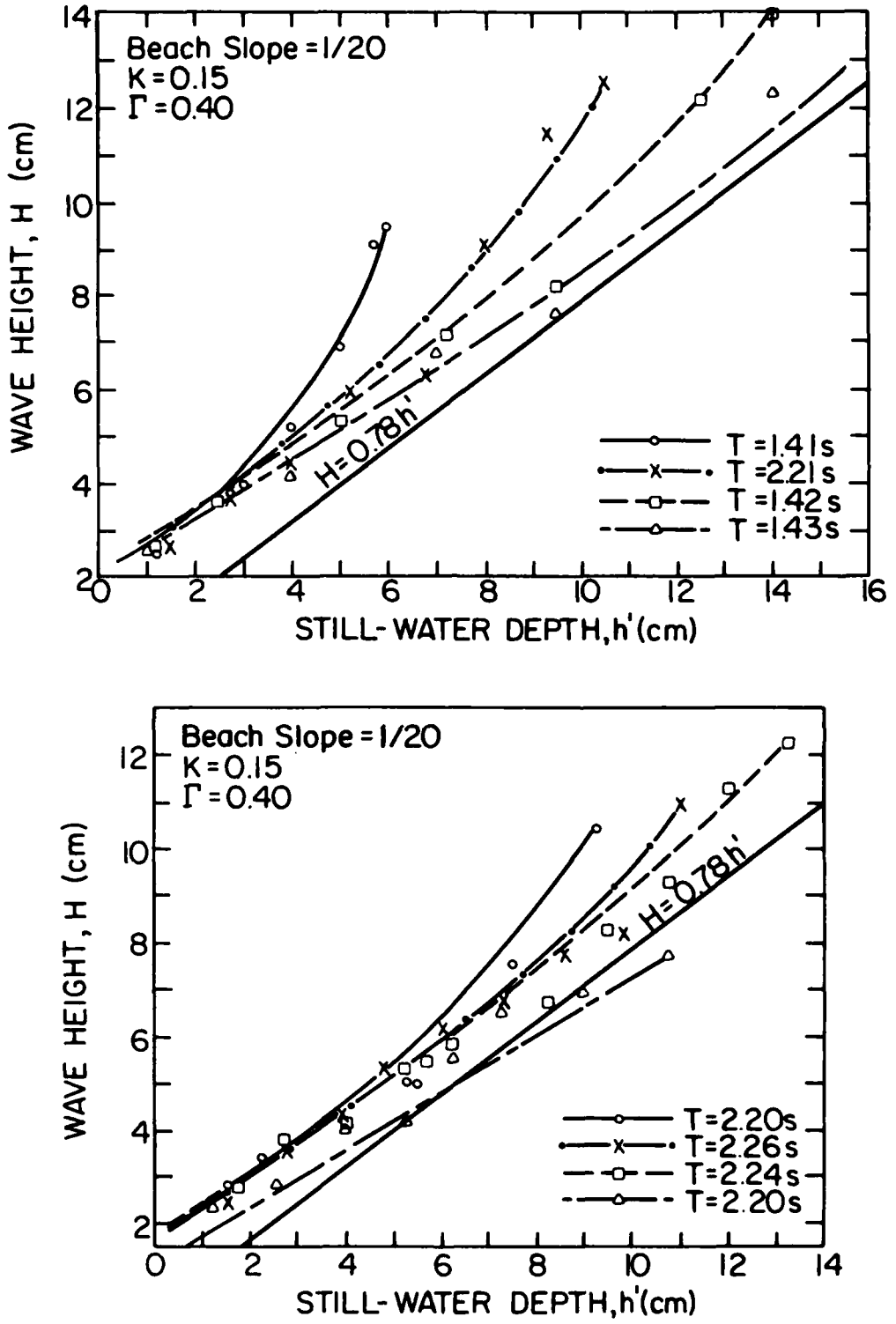

Figure 11. Comparison of breaker model and 0.78 criterion with the laboratory data of Horikawa and Kuo for 1/20 beach slope

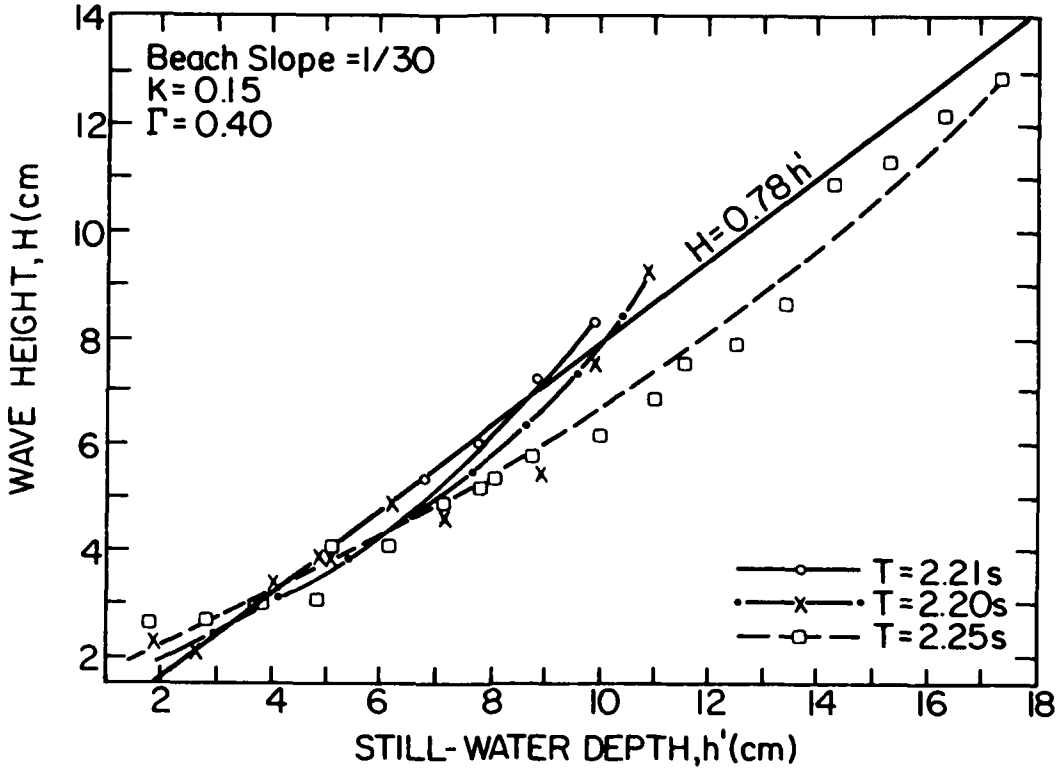

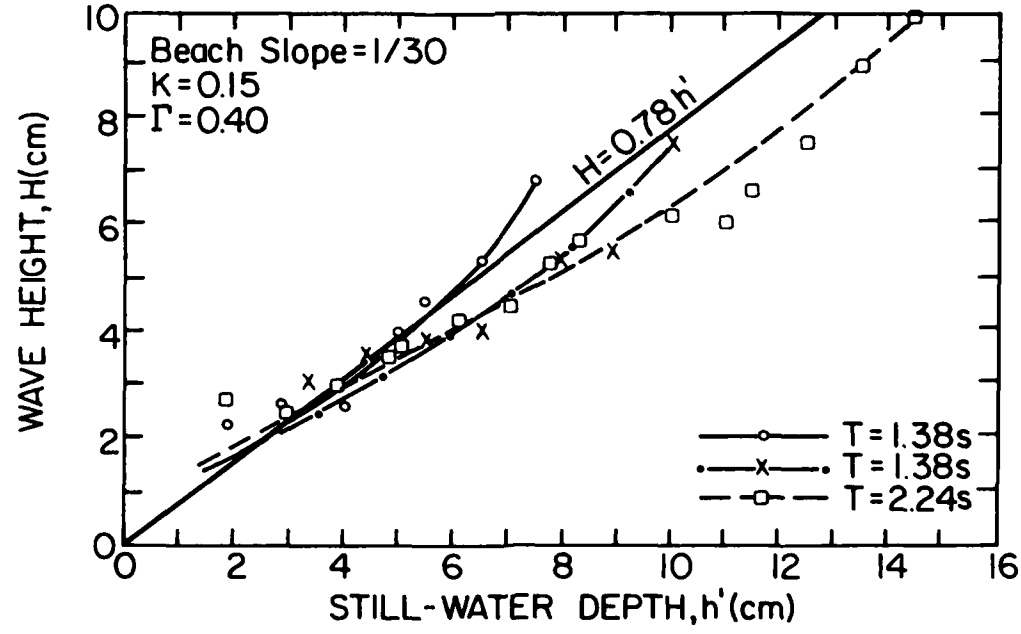

Figure 12. Comparison of breaker model and 0.78 criterion with the laboratory data of Horikawa and Kuo for 1/30 beach slope

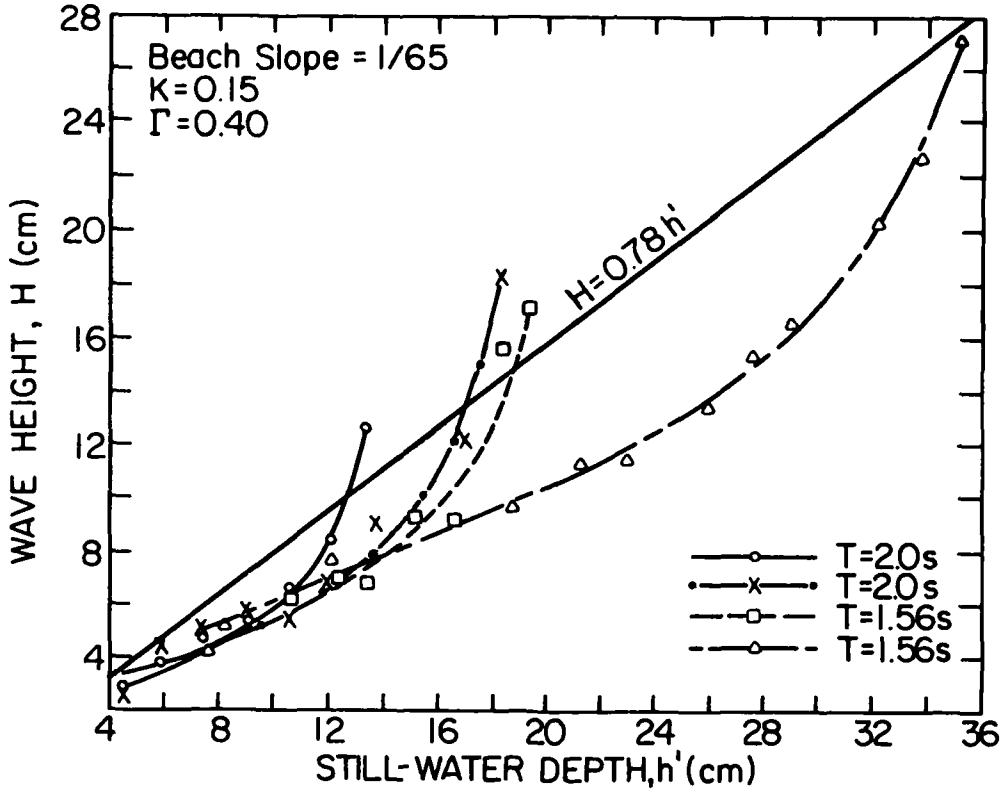

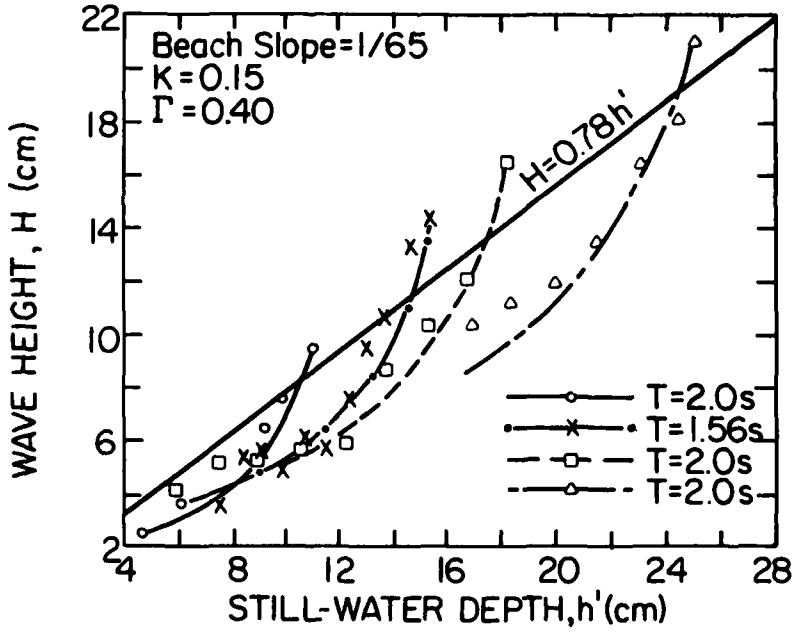

Figure 13. Comparison of breaker model and 0.78 criterion with the laboratory data of Horikawa and Kuo for 1/65 beach slope

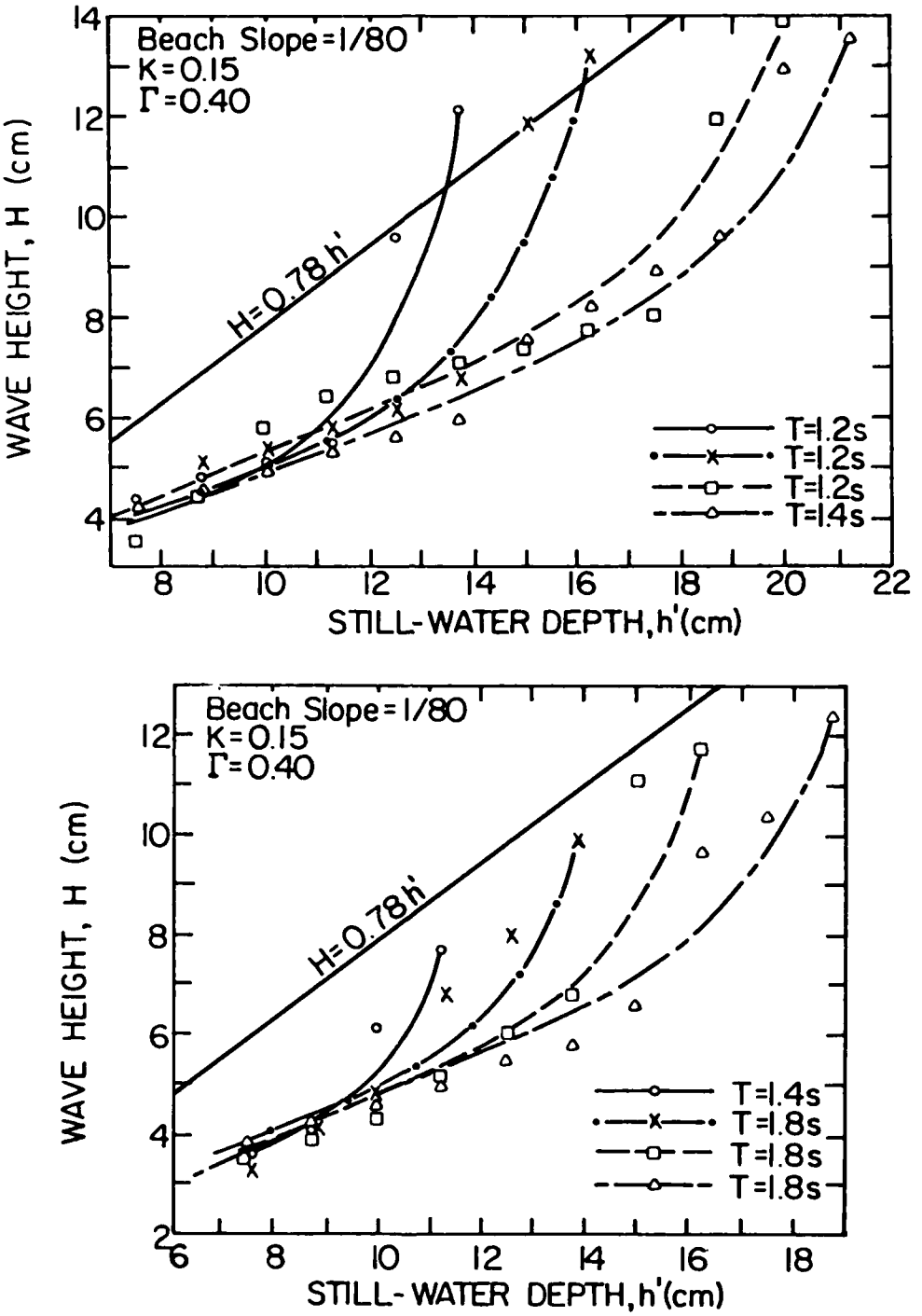

Figure 14. Comparison of breaker model and 0.78 criterion with the laboratory data of Horikawa and Kuo for 1/80 beach slope

28. Although the range in wave period in the data is limited (1.2 - 2.26 sec), it appears that wave period is not a primary factor in the decay of wave height after breaking is initiated due to the fact that breaking is a phenomenon restricted only to a portion of the wave crest. Wave period does affect the wave-height-to-water-depth ratio at incipient breaking (along with beach shape, slope, and deepwater wave height) and therefore affects the shape of the decay profile through the initial condition. Wave period plays no direct role in the decay portion of the present model because the incipient conditions are given as input to the model.

29. Characteristically, waves of the plunging type dissipate a large portion of their energy in a concentrated manner in the region just shoreward of the breaker line, while spilling breakers dissipate their energy at a slower rate. At incipient breaking, the wave-height-to-depth ratio is usually greater than 1.0 for plunging breakers and 0.78 or less for spilling breakers. Figure 15 presents predicted wave height decay curves for two waves with the same initial breaking depth but different wave heights. The larger wave initially decays at a much greater rate than the smaller, and it appears the model is at least qualitatively correct in dealing with the breaker types, plunging and spilling.

30. Figure 16 demonstrates the negligible effect energy losses from bottom friction have on the wave decay profile when compared to breaking. The upper curve is a test case of the model without bottom friction. The lower curve was generated with the same conditions, except greatly exaggerated bottom friction losses (assuming no bed form losses) were included. The drag coefficient f for the bottom was set equal to 0.10, about two orders of magnitude greater than is realistic for the smooth rubber and concrete slopes used by Horikawa and Kuo. This was for the purpose of distinguishing between the two curves.

Setup

31. The data of Horikawa and Kuo do not include measurements of setup, so experimental data presented in Bowen, Inman, and Simmons (1968) and Bowen (1969) were examined. In these experiments wave heights and mean water levels were measured on a relatively steep plane beach of 1/12 slope. The results of two tests are presented in Figures 17 and 18, along with the decay and setup

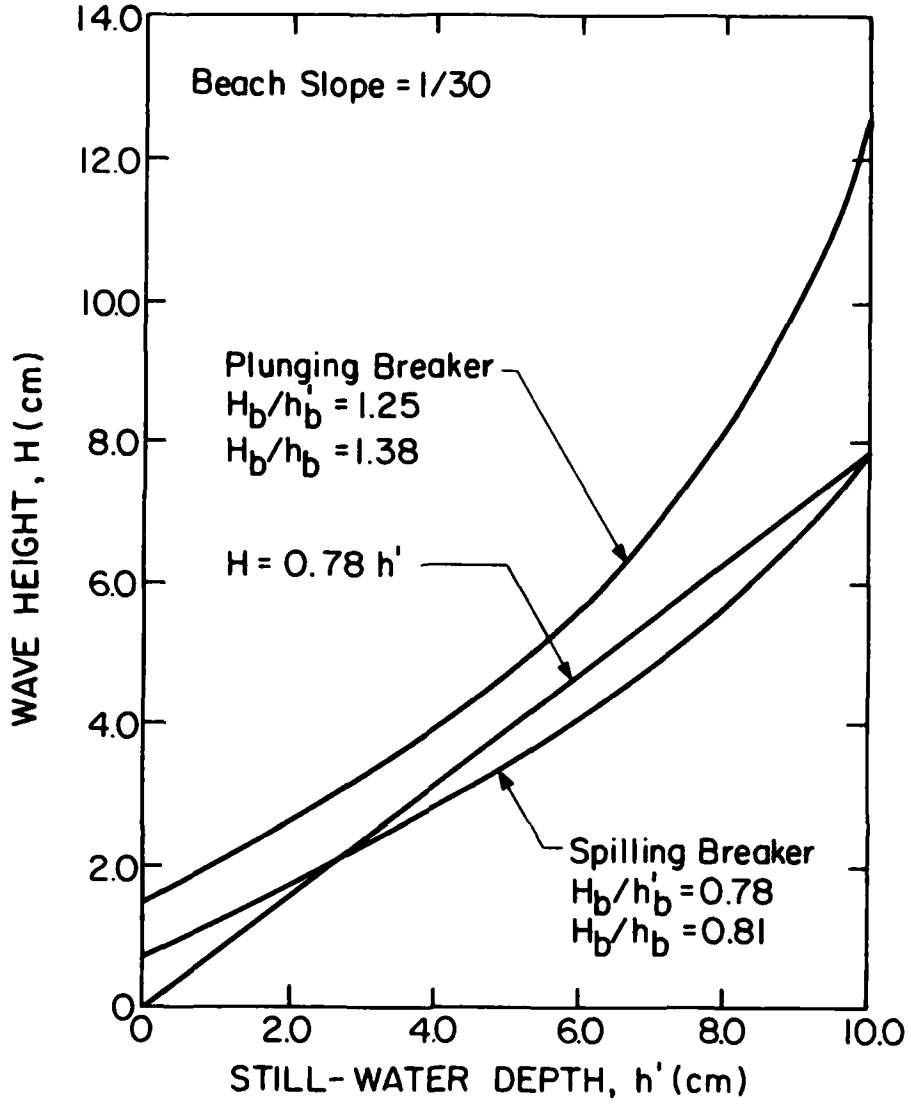

Figure 15. Comparison of model-predicted wave decay for spilling and plunging breakers

curves predicted by the numerical model (K = 0.25 , Γ = 0.35). The breaker decay compares well and the maximum setup values are reasonable if swash zone is neglected; however, the predicted setup curves do not follow the data. Apparently, Equation 20 is not a good representation of the onshore excess momentum flux for near-breaking and breaking conditions as might be expected. Higher order wave theories yield significantly less momentum flux for a given wave height than linear theory (Dean 1974), and this difference is the most likely explanation for the discrepancy between the measured and predicted setup profiles.

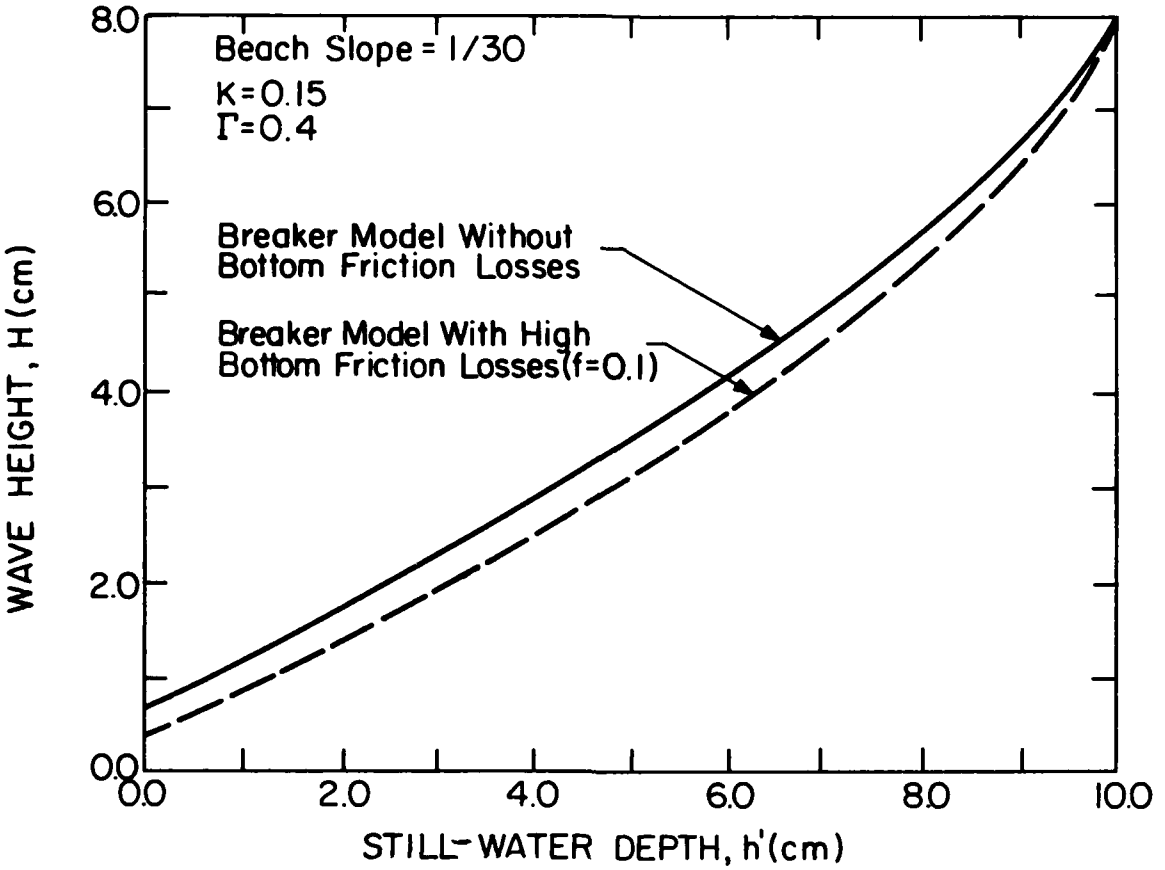

Figure 16. Comparison of model-predicted wave decay with and without bottom friction losses

32. As noted by Bowen, Inman, and Simmons (1968), the measured setdown is nearly uniform in the region between incipient breaking and the point where the curl of the plunging breaker touches down. It is interesting that even though the wave height is decreasing in this region, the momentum flux apparently is not. Perhaps this is because (strictly speaking) no energy is dissipated until the curl touches down and "white water" appears.

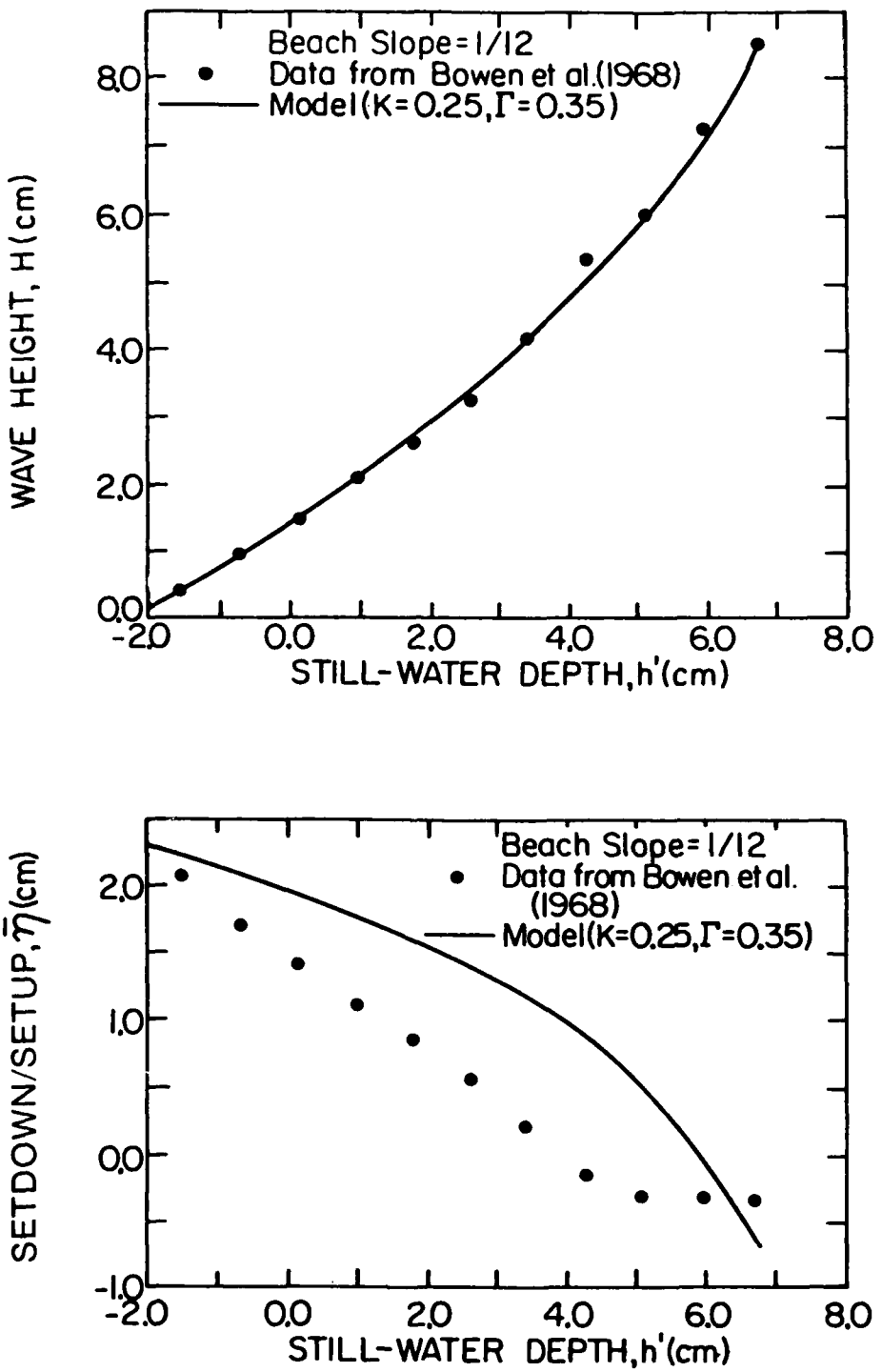

Figure 17. Model-predicted wave decay and setdown/setup as compared with laboratory data from Bowen, et al. (1968)

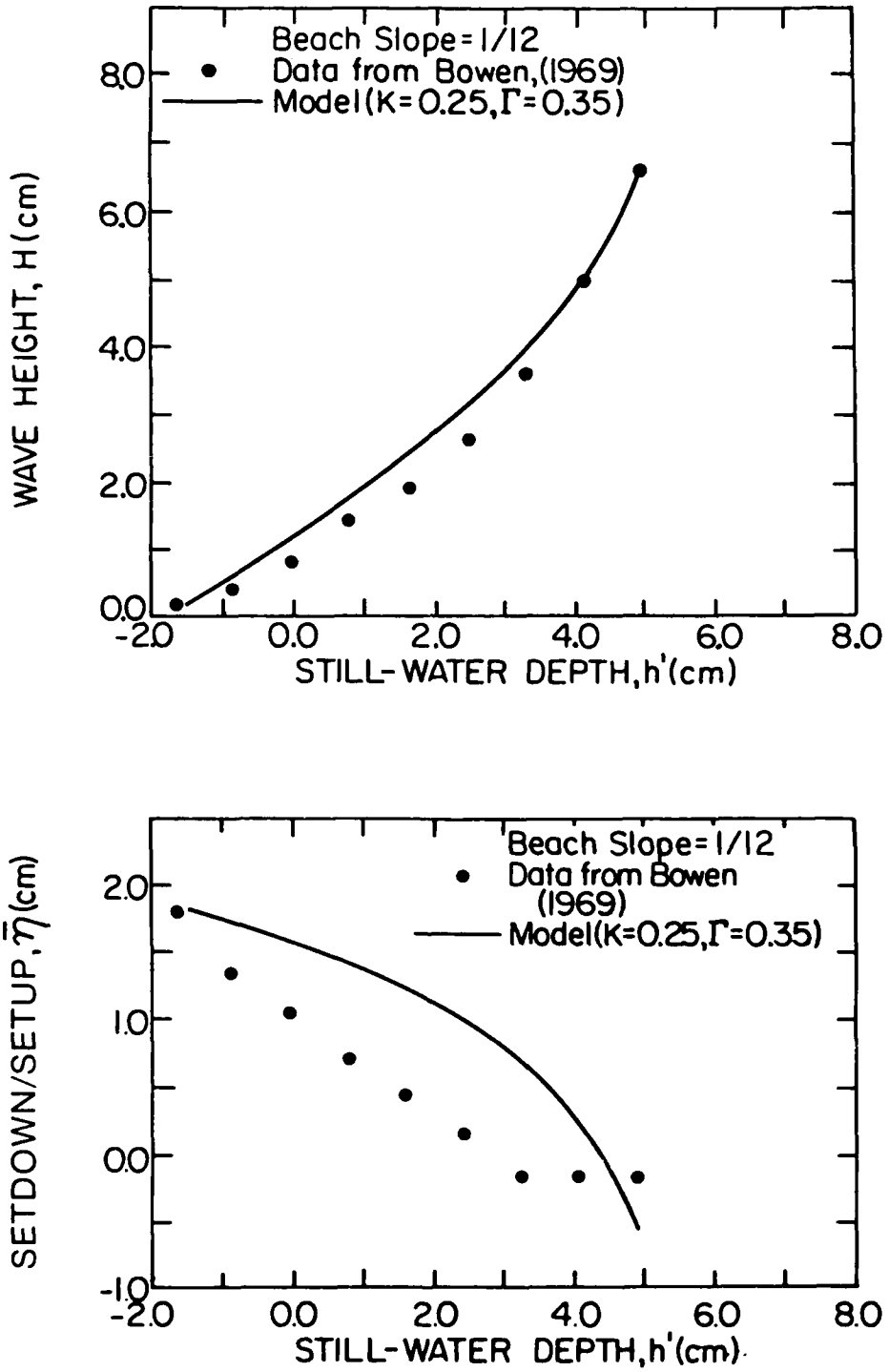

Figure 18. Model-predicted wave decay and setdown/setup as compared with laboratory data from Bowen (1969)

PART IV: RESULTS FOR LARGE SCALE CONDITIONS

33. Applying the results of the laboratory calibration to near-prototype conditions may be questionable due to expected scale effects in the turbulence associated with wave breaking as previously discussed. However, in order to demonstrate use of the model for waves breaking on beach profiles containing bars and to lend some validity to the model for prototype situations, the model was run for large scale conditions. A "prototype scale" beach profile generated by Saville (1957) in the Beach Erosion Board's large wave tank was utilized and is displayed in Figure 19. The profile is characterized by three offshore bar/trough systems, along with a monotonic section in the nearshore region. Test conditions, although sketchy, were taken from the laboratory notes as

Wave period, $T = 11.33$ sec

Wave height at incipient breaking, $H_b = 1.78$ m

Location of outside breaker line = 76.8 m from still-water line on beach

Mean sediment diameter, $D = 0.2$ mm

These conditions placed the breaker line outside the crest of the first bar at a still-water depth of 1.78 m. The setdown in mean water level given by Equation 36 is -0.11 m, and the ratio of wave height to mean water depth at incipient breaking is 1.07. Γ was set equal to 0.4, and, because the seaward faces of the bars were steep, K was set equal to 0.2. Following the procedure described by Kamphuis (1975) and assuming the bottom was not rippled, the bottom friction factor f was found to be roughly 0.005. Initial runs showed that bottom friction caused decay on the order of millimeters only. Apparently, bottom friction plays an important role in wave decay only under non-breaking conditions well outside the surf zone, and friction was again left out of the model for this test. Using these incipient conditions, the transformation of wave height was generated in a stepwise fashion across the entire surf zone ($\Delta x = 1.5$ m) until the mean water depth became less than 0.25 m. The distribution of model-predicted wave height and setup are also shown in Figure 19. Note that the wave reaches the stable criterion in the outermost trough as might be expected, but does not shoal enough on the second bar to

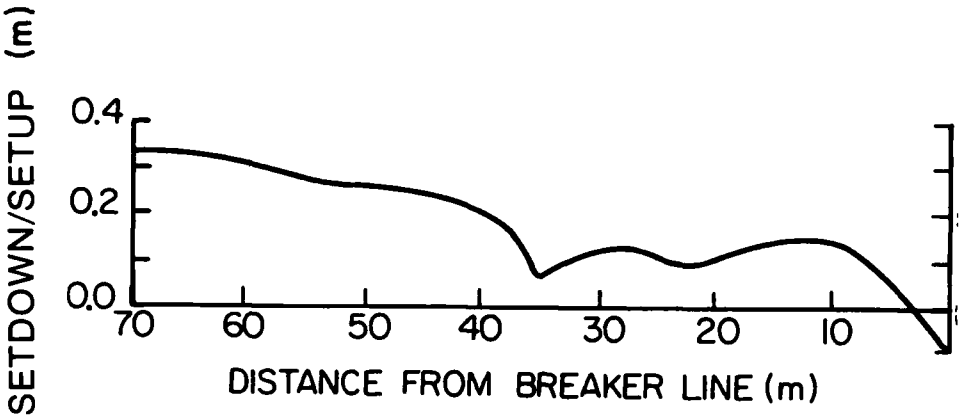

a. Setdown/setup

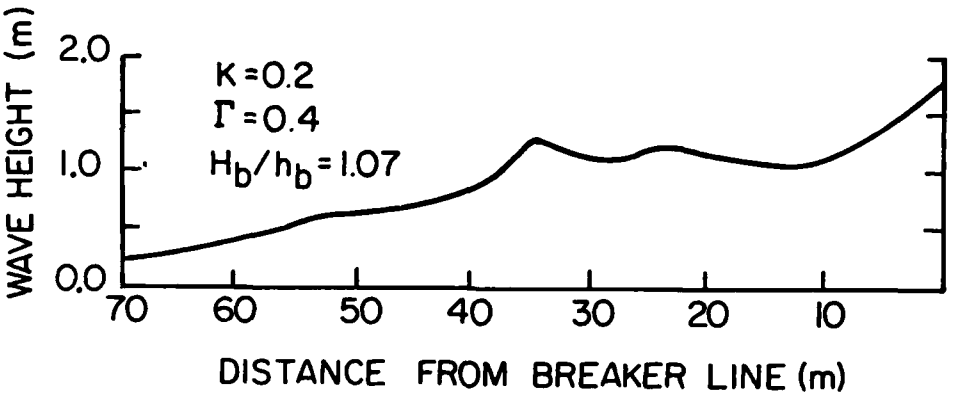

b. Wave decay

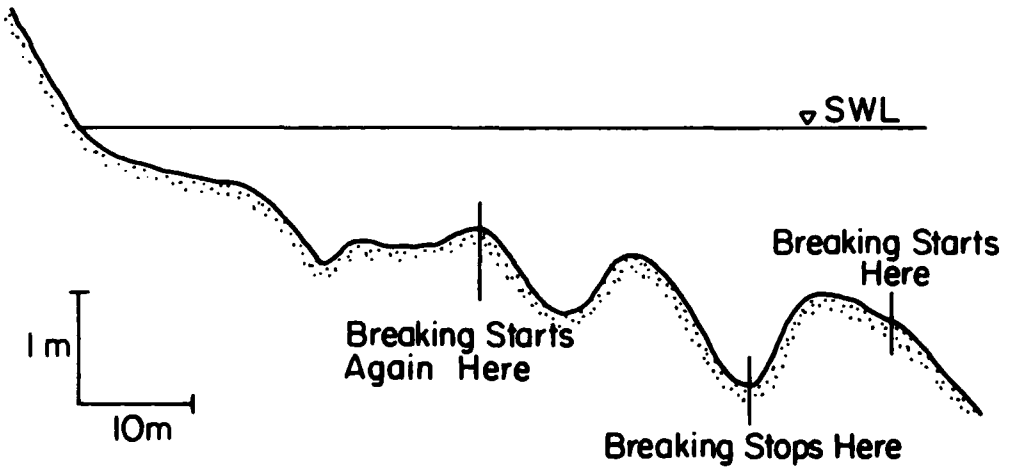

c. Bottom profile

Figure 19. Test of wave transformation model at prototype scale on large wave tank profile from Saville (1957)

reach the incipient breaking criterion. Instead, it continues past the second trough (losing magnitude slightly due to the deeper water) until the third bar is encountered where breaking starts again and continues until the shoreline is reached.

34. The results of application of the model under large scale conditions seem reasonably valid, at least in a qualitative sense. The example has demonstrated the ability of the model to describe wave breaking and reformation, a commonly observed process on natural beaches. The predicted wave decay and setup profiles are continuous and well-behaved until the mean water depth becomes quite small ($h < 0.25$ m), where a swash zone model might be more appropriate.

PART V: CONCLUSIONS AND RECOMMENDATIONS

35. Based on laboratory data collected by Horikawa and Kuo (1966), the parameters found to affect most the decay in wave height due to breaking in the surf zone are the wave-height-to-water-depth ratio at incipient breaking and the beach slope. Wave-induced setup in mean water level plays a smaller but non-trivial role in governing the shape of the wave decay profile, especially near the still-water line. The similarity model $H \propto h'$ commonly used by the coastal profession, appears to be reasonable only on steep beaches (1/20 to 1/30 at laboratory scale), and the 0.78 criterion predicts with marginal accuracy for a 1/30 slope only. However, the model developed herein appears to qualitatively and quantitatively describe wave transformation in the surf zone due to shoaling, breaking, and reformation over a wide range of beach slopes (1/80 to 1/12) and incipient conditions ($0.63 \leq (H/h_b) \leq 1.67$). Its greatest assets are its simplicity and ease of application. Although it is most successful on profiles of monotonic shape, it may also be employed when multiple bar/trough systems are present.

36. The model predicts maximum setup values with reasonable accuracy for two test cases presented by Bowen, Inman, and Simmons (1968) and Bowen (1969); however, it does not describe the distribution of setup across the surf zone satisfactorily. Apparently, the basic assumption that onshore radiation stress can be described by using linear wave theory is not a valid one under near-breaking conditions. More work is required in this area.

37. From calculations based on the work of Kamphuis (1975), it can be concluded that bottom friction plays a negligible role in wave decay in the surf zone for most naturally occurring conditions when compared with the effects of breaking and shoaling. Bottom friction could be significant in nearshore regions that have very mild slopes or rough bottoms.

38. The model has certain limitations which might restrict its use. Reflection is not included, and, although the model appears valid even for a 1/12 slope, one must be careful when interpreting results for runs on steep beaches. An elementary scheme utilizing reflection coefficients might be included. A breaking phenomenon not handled well by the model is wave "tripping" which commonly occurs when incipient breaking conditions are reached at or near the peak of a bar or submerged structure and the wave travels onto the trough before breaking becomes fully developed. The model might be improved

by including also the transfer of energy to higher frequencies as studied by Sawaragi and Iwata (1974). However, the cause of this phenomenon is not fully understood at present. To better represent natural conditions, another logical improvement would be an application to random waves, perhaps similar to the analysis of Battjes and Janssen (1978) or Thornton and Guza (1983).

REFERENCES

Battjes, J. A., and Janssen, J. P. F. M. 1978. "Energy Loss and Set-up Due to Breaking of Random Waves," Proceedings, Sixteenth Conference on Coastal Engineering, American Society of Civil Engineers, Vol 1, pp 569-587.

Bowen, A. J., Inman, D. L., and Simmons, V. P. 1968. "Wave Set-Down and Set-Up," Journal of Geophysical Research, Vol 73, No. 8, pp 2569-2577.

Bowen, A. J. 1969. "Rip Currents, 1: Theoretical Investigations," Journal of Geophysical Research, Vol 74, pp 5467-5478.

Collins, J. I. 1970. "Probabilities of Breaking Wave Characteristics," Proceedings, Twelfth Conference on Coastal Engineering, American Society of Civil Engineers, Vol 1, pp 399-412.

Dean, R. G. 1974. "Evaluation and Development of Water Wave Theories for Engineering Application," US Army Coastal Engineering Research Center, Special Report No. 1.

Divoky, D., Le Méhauté, B. and Lin, A. 1970. "Breaking Waves on Gentle Slopes," Journal of Geophysical Research, Vol 75, No. 9, pp 1681-1692.

Goda, Y. 1975. "Irregular Wave Deformation in the Surf Zone," Coastal Engineering in Japan, Vol 18, pp 13-26.

Horikawa, K., and Kuo, C. T. 1966. "A Study of Wave Transformation Inside Surf Zone," Proceedings, Tenth Conference on Coastal Engineering, American Society of Civil Engineers, Vol 1, pp 217-233.

Hwang, L. S., and Divoky, D. 1970. "Breaking Wave Set-Up and Decay on Gentle Slopes," Proceedings, Twelfth Conference on Coastal Engineering, American Society of Civil Engineers, Vol 1, pp 377-389.

Kamphuis, J. W. 1975. "Friction Factor Under Oscillatory Waves," Journal of the Waterways and Harbors Division, American Society of Civil Engineers, Vol 101, No. WW2, pp 135-144.

Kuo, C. T., and Kuo, S. T. 1974. "Effect of Wave Breaking on Statistical Distribution of Wave Heights," Proceedings, Civil Engineering in the Oceans III, American Society of Civil Engineers, Vol 2, pp 1211-1231.

Lamb, H. 1932. Hydrodynamics, 6th ed., Cambridge University Press, Cambridge, England.

Le Méhauté, B. 1962. "On Non-Saturated Breakers and the Wave Run-up," Proceedings, Eighth Conference on Coastal Engineering, American Society of Civil Engineers, pp 77-92.

Longuet-Higgins, M. S., and Stewart, R. W. 1963. "A Note on Wave Set-Up," Journal of Marine Research, Vol 21, pp 4-10.

Mallard, W. W. 1978. "Investigation of the Effect of Beach Slope on the Breaking Height to Depth Ratio," Master's Thesis, Department of Civil Engineering, University of Delaware, Newark, Del.

Mizuguchi, M. 1980. "An Heuristic Model of Wave Height Distribution in Surf Zone," Proceedings, Seventeenth Coastal Engineering Conference, American Society of Civil Engineers, Vol 1, pp 278-289.

Nakamura, M., Shiraishi, H., and Sasaki, Y. 1966. "Wave Decaying Due to Breaking," Proceedings, Tenth Conference on Coastal Engineering, American Society of Civil Engineers, Vol 1, pp 234-253.

Peregrine, D. H., and Svendsen, I. A. 1978. "Spilling Breakers, Bores, and Hydraulic Jumps," Proceedings, Sixteenth Conference on Coastal Engineering, American Society of Civil Engineers, Vol 1, pp 540-550.

Saville, T. 1957. "Scale Effects in Two-Dimensional Beach Studies," Transactions of the Seventh Meeting of the International Association for Hydraulic Research, pp A3.1-A3.10.

Sawaragi, T., and Iwata, K. 1974. "On Wave Deformation After Breaking," Proceedings, Fourteenth Conference on Coastal Engineering, American Society of Civil Engineers, Vol 1, pp 481-497.

Street, R. L., and Camfield, F. E. 1966. "Observations and Experiments on Solitary Wave Deformation," Proceedings, Tenth Conference on Coastal Engineering, American Society of Civil Engineers, Vol 1, pp 284-293.

Svendsen, I. A., et al. 1978. "Wave Characteristics in the Surf Zone," Proceedings, Sixteenth Conference on Coastal Engineering, American Society of Civil Engineers, Vol 1, pp 520-539.

Thornton, E. B., and Guza, R. T. 1983. "Transformation of Wave Height Distribution," Journal of Geophysical Research, Vol 88, No. C10, pp 5925-5938.

APPENDIX A: ANALYTICAL SOLUTIONS FOR THE BREAKING WAVE MODEL

Horizontal Bottom

1. The proposed expression (Equation 10) for predicting wave decay due to breaking in the surf zone (wave-induced setup and bottom friction not included) can be solved analytically for the flat shelf case shown in Figure 1b. Starting with Equation 10*

$$\frac{d(ECg)}{dx} = \frac{-K}{h'} [ECg - (ECg)_s] \tag{A1}$$

making the "stable wave" assumption

$$H_s = \Gamma h' \tag{A2}$$

and applying linear shallow-water wave theory, the expression takes the form

$$h'^{1/2} \frac{dH^2}{dx} = \frac{-K}{h'} (H^2 h'^{1/2} - \Gamma^2 h'^{5/2}) \tag{A3}$$

Letting $F = H^2$ and rearranging yields

$$\frac{dF}{dx} + \frac{K}{h'} F = K\Gamma^2 h' \tag{A4}$$

This first-order ordinary differential equation is solved by summing a homogeneous solution and a particular solution, or

$$F = F_H + F_P \tag{A5}$$

The homogeneous solution obtained from

$$\frac{dF_H}{dx} + \frac{K}{h'} F_H = 0 \tag{A6}$$

---

* For convenience, symbols and unusual abbreviations are listed and defined in the Notation (Appendix B).

is given by

$$F_H = Ae^{-Kx/h'} \tag{A7}$$

where A is an arbitrary coefficient. Let the particular solution F_p be a constant C and from Equation A4

$$C = \Gamma^2 h'^2 \tag{A8}$$

and the complete solution has the form

$$F = Ae^{-Kx/h'} + \Gamma^2 h'^2 \tag{A9}$$

Applying the boundary condition at the breaker line

$$F = F_b = H_b^2 \text{ at } x = 0 \tag{A10}$$

the coefficient A is determined

$$A = H_b^2 - \Gamma^2 h'^2 \tag{A11}$$

and the solution becomes

$$H^2 = \left(H_b^2 - \Gamma^2 h'^2\right) e^{-Kx/h'} + \Gamma^2 h'^2 \tag{A12}$$

or

$$\frac{H}{h'} = \left(\left\{ \left[\left(\frac{H}{h'}\right)_b^2 - \Gamma^2 \right] \exp \left(\frac{-Kx}{h'}\right) \right\} + \Gamma^2 \right)^{1/2} \tag{A13}$$

Plane Beach

2. For the case of a plane beach described by the expression

$$h' = h_b' - mx \tag{A14}$$

where the origin is again at the breaker line and x directed onshore, Equation 8 can be solved analytically again. Following the same procedure as for the horizontal bottom case, the following equation is developed

$$\frac{dG}{dx} + \frac{K}{h'} G = K\Gamma^2 h'^{3/2} \tag{A15}$$

where $G = H^2 h'^{1/2}$. Converting the derivative with respect to distance to a derivative with respect to still-water depth by utilizing Equation A14 yields

$$\frac{dG}{dh'} - \frac{K}{mh'} G = \frac{-K\Gamma^2}{m} h'^{3/2} \tag{A16}$$

Let the solution to the homogeneous equation

$$\frac{dG_H}{dh'} - \frac{K}{mh'} G_H = 0 \tag{A17}$$

have the form

$$G_H = Ah'^n \tag{A18}$$

where A and n are arbitrary constants. Substituting into Equation A17 produces

$$A\left(nh'^{n-1} - \frac{K}{m} h'^{n-1}\right) = 0 \tag{A19}$$

In order for the homogeneous solution to be non-trivial, $n = K/m$ and

$$G_H = Ah'^{K/m} \tag{A20}$$

Let the particular solution have the form

$$G_P = Bh'^{\,n} \tag{A21}$$

where B and n are arbitrary constants. From Equation A16

$$B\left(nh'^{n-1} - \frac{K}{m}h'^{n-1}\right) = \frac{-K\Gamma^2}{m}h'^{3/2} \tag{A22}$$

For the equality to hold for all values of h', $n = 5/2$ and therefore

$$B = \frac{-K\Gamma^2}{m\left(\frac{5}{2} - \frac{K}{m}\right)} \tag{A23}$$

and

$$G = Ah'^{K/m} - \frac{K\Gamma^2}{m\left(\frac{5}{2} - \frac{K}{m}\right)}h'^{5/2} \tag{A24}$$

The coefficient A is determined by applying the boundary condition

$$G = G_b = H_b^2 h_b'^{1/2} \text{ at } h' = h_b' \tag{A25}$$

and

$$A = \frac{H_b^2 h_b'^{1/2}}{h_b'^{K/m}} + \frac{K\Gamma^2 h_b'^{5/2}}{m\left(\frac{5}{2} - \frac{K}{m}\right)h_b'^{K/m}} \tag{A26}$$

Substituting into Equation A24 and putting the result into dimensionless form

$$\frac{H}{H_b} = \left[\left(\frac{h'}{h'_b} \right)^{[(K/m)-1/2]} (1 + \alpha) - \alpha \left(\frac{h'}{h'_b} \right)^2 \right]^{1/2} \tag{A27}$$

where

$$\alpha = \frac{K\Gamma^2}{m\left(\frac{5}{2} - \frac{K}{m}\right)} \left(\frac{h'}{H} \right)_b^2 \tag{A28}$$

Note that if $K/m = 5/2$, the solution fails. For this case let the particular solution have the form

$$G_p = V(h')h'^{5/2} \tag{A29}$$

and from Equation A16 we find

$$V(h') = -\frac{5}{2} \Gamma^2 \ell n\, h' \tag{A30}$$

and the total solution is now

$$G = Ah'^{5/2} - \frac{5}{2} \Gamma^2 h'^{5/2} \ell n\, h' \tag{A31}$$

Applying the same boundary condition as before yields

$$A = \frac{H}{h'}_b^2 + \frac{5}{2} \Gamma^2 \ell n\, h'_b \tag{A32}$$

and the final result in dimensionless form for the special case of $K/m = 5/2$ is

$$\frac{H}{H_b} = \left(\frac{h'}{h'_b}\right) \left[1 - \beta \ \ell n\left(\frac{h'}{h'_b}\right)\right]^{1/2} \tag{A33}$$

where

$$\beta = \frac{5}{2} \Gamma^2 \left(\frac{h'}{H}\right)_b^2 \tag{A34}$$

APPENDIX B: NOTATION

C_g	group velocity
E	wave energy per unit surface area
E_{flux}	energy flux
E'	specific energy of flow
f	drag coefficient (bottom friction factor)
$\mathbb{F}$	Froude number
g	acceleration due to gravity, constant
h	mean water depth including setup
h'	still-water depth
H	wave height
K	dimensionless decay coefficient, wave decay factor
m	beach slope
t	time
T	wave period
u	horizontal fluid velocity
x	horizontal coordinate
γ	unit weight of water
Γ	dimensionless coefficient (about 0.35 - 0.40), stable wave factor
Δx	size of numerical step
ε	error function
$\bar{\eta}$	setup
ρ	mass density of water

Subscripts

b	corresponds to incipient breaking
s	corresponds to stable wave

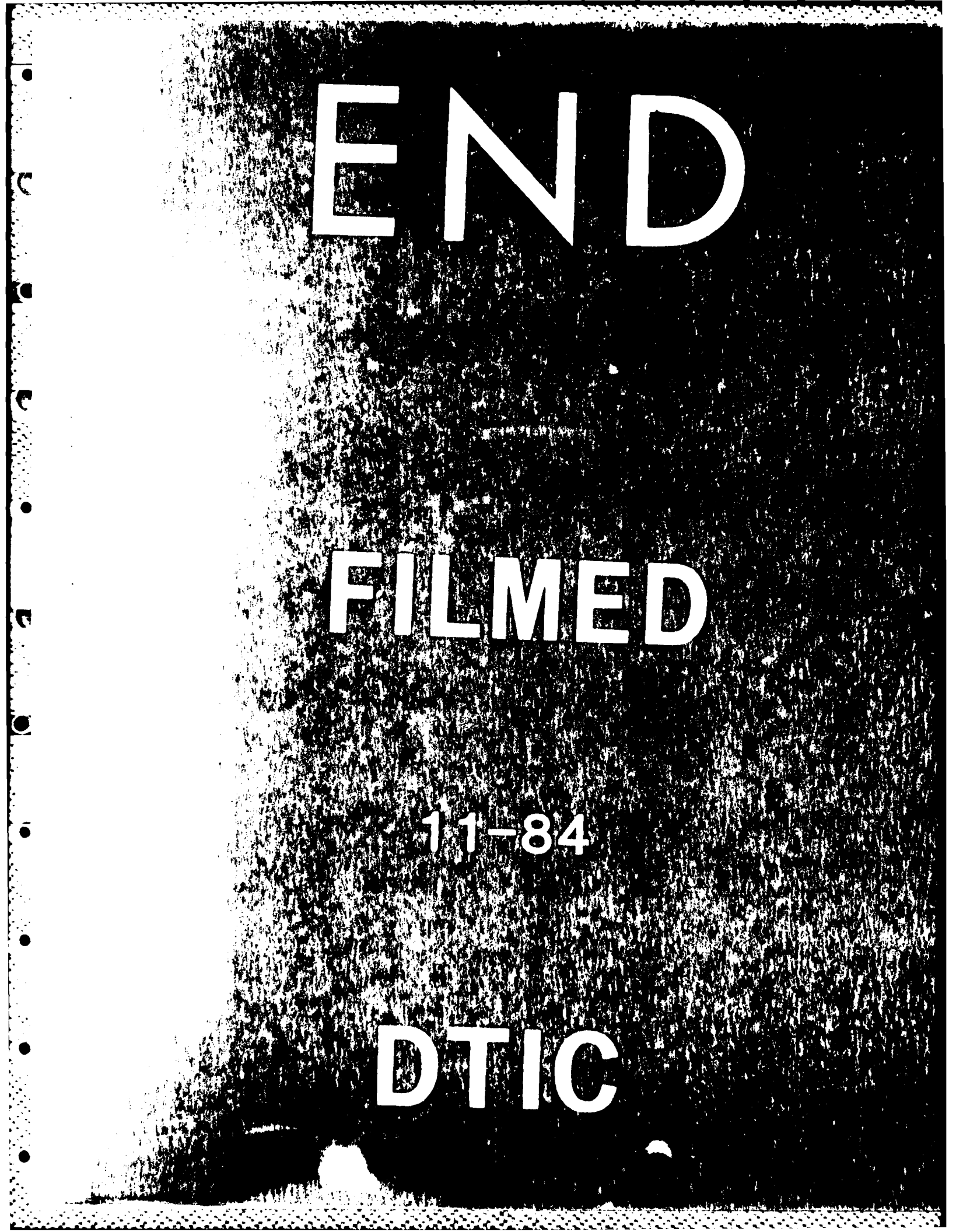
END
FILMED
11-84
DTIC